NTNU – Trondheim
Norwegian University of
Science and Technology

Vibrations in Composite Timber-Concrete Floor Systems

Mathilde Korvald Skaare

Norwegian University of Science and Technology
Department of Structural Engineering

Department of Structural Engineering
Faculty of Engineering Science and Technology
NTNU- Norwegian University of Science and Technology

MASTER THESIS 2013

SUBJECT AREA:	DATE:	NO. OF PAGES:
CONSTRUCTION	08.06.13	83

TITLE:

Vibrations in composite timber-concrete floor systems

Vibrasjoner i etasjeskiller av kompositt i tre og betong

BY:

MATHILDE KORVALD SKAARE

SUMMARY:

Timber-concrete composite structures were originally developed for bridges and strengthening existing timber floors, but is today used extensively also in new buildings. The objective of this thesis was to look at the dynamic behaviour of a timber-concrete composite system.

A full-scale model was built in the laboratory, and the following tests were performed: A dynamic test (hammer impact test) and a deflection test with 1 kN load. In addition a direct shear test was performed on two asymmetrical specimens to find the stiffness of the shear connector. There was also made a numerical model in ABAQUS, to estimate the behaviour of the composite beam.

The hammer impact test showed that the composite beam satisfied the dynamic requirements sat for the beam. The shear connector proved to be weaker and more ductile than expected. It was discovered this was due to insufficient gluing during the assembly. The numerical analyses done in combination with the empirical tests proved to give good estimates on the behaviour of the composite beam. The stiffness of the shear connector proved to be more decisive of the deflection of the beam than the frequency. Expanding the beam to a full-size floor in ABAQUS indicated that the composite beam gave smaller values for the frequency than what would be the case for a full floor.

The overall performance of the timber-concrete composite system tested in this thesis was good. However, some adjustments should be made and more research has to be done, if developing this into a new floor system.

RESPONSIBLE TEACHER: KJELL ARNE MALO

SUPERVISOR(S) KJELL ARNE MALO, TERJE KANSTAD

CARRIED OUT AT: DEPARTMENT OF STRUCTURAL ENGINEERING

Institutt for konstruksjonsteknikk
FAKULTET FOR INGENIØRVITENSKAP OG TEKNOLOGI
NTNU – Norges teknisk-naturvitenskapelige universitet

MASTEROPPGAVE 2013

for

Mathilde Korvald Skaare

Vibrasjoner i etasje-skiller av kompositt i tre og betong.

Vibrations in composite timber-concrete floor systems

Tre er et sterkt, men lett byggemateriale og det kan settes i svingninger både av rytmisk menneskelig aktivitet som gange og dans, så vel som av vindbelastning. I denne oppgaven vil vi benytte etasjeskillere sammensatt hovedsakelig av trebaserte bjelker med trykksone i betongmaterialer som studieobjekt. Ønskede egenskaper til etasjeskiller er mest knyttet til vibrasjoner forårsaket av bevegelse av personer eller maskiner og lydskillende egenskaper primært mellom forskjellige boenheter. Som et bidrag til utvikling av bedre etasjeskillere basert på bruk av tre og trekonstruksjoner i samvirke med andre materialer, gjennomføres det prosjekter hvor med både eksperimentelle forsøk og numeriske simuleringer med elementmetoden (Abaqus) inngår. Hensikten med dette arbeidet er å se på muligheten for å benytte lengre spennvidder ved å introdusere komposittløsninger, noe momentinnspenning ved endene og noe mere dempning. Numeriske simuleringer og eksperimentelle resultater benyttes i parallell for å klarlegge hvordan slike etasjeskillere bør konstrueres for å gi gode resultater.

Forutsetninger:

De eksperimentelle modellene skal detaljprosjekteres og bygges i laboratoriet.

Etter samråd med veiledere kan kandidatene konsentrere sitt arbeide til spesielle deler av oppgaven, eller trekke inn andre aspekter.

Besvarelsen organiseres i henhold til gjeldende retningslinjer.

Veileder(e):   Kjell Arne Malo og Terje Kanstad

Besvarelsen skal leveres til Institutt for konstruksjonsteknikk innen 10. juni 2013.

NTNU, 14. januar , 2013

Kjell Arne Malo
faglærer

Preface

This is a MSc thesis written for the Department of Structural Engineering at the Norwegian University of Science and Technology (NTNU) in Trondheim. The work has been accomplished during 20 effective weeks in the spring of 2013.

The thesis discusses the use of timber-concrete composite structures in floors, and their dynamic behaviour. This is a field that was mostly uknown for me 20 weeks ago, and the process of this thesis has therefore been very instructive and inspiring. The combination of laboratory work and numerical analyses has made the work varying, with some hectic periods along the way.

I would first of all like to thank my supervisor Professor Kjell Arne Malo, who not only put me on the idea of this thesis, but also has been supportive the whole way. His door is always open for questions and discussions, and his enthusiasm is encouraging.

The same can be said about Professor Terje Kanstad, who has supervised me on the concrete part. He has with great interest followed the work on this thesis, and help was never far away.

Many hours has been spent in the laboratory this semester. I would never been able to build the model if it was not for the exceptional help from the staff there, especially Steinar Seehus, Ragnar Moen, Gøran Loraas and Per Øystein Nordtug. Their experience and support have been very valuable, thank you!

Trondheim, June 8, 2013

Mathilde Korvald Skaare

Abstract

Timber-concrete composite structures were originally developed for bridges and strengthening existing timber floors, but is today used extensively also in new buildings. The objective of this thesis was to look at the dynamic behaviour of a timber-concrete composite system, where the concrete deck consisted of several prefabricated elements glued together. The shear connector used was a glued-in steel mesh, which had shown strong capacity in previous studies. The concrete was fibre reinforced concrete.

A full-scale model was built in the laboratory, and the following tests were performed: A dynamic test (hammer impact test) and a deflection test with 1 kN load. In addition a direct shear test was performed on two asymmetrical specimens to find the stiffness of the shear connector. The fibre reinforced concrete was tested separately to find its characteristic properties. There was also made a numerical model in ABAQUS, to estimate the behaviour of the composite beam.

The hammer impact test showed that the composite beam satisfied the dynamic requirements sat for the beam. The shear connector proved to be weaker and more ductile than expected. It was discovered this was due to insufficient gluing during the assembly. The numerical analyses done in combination with the empirical tests proved to give good estimates on the behaviour of the composite beam. The stiffness of the shear connector proved to be more decisive of the deflection of the beam than the frequency. Expanding the beam to a full-size floor in ABAQUS indicated that the composite beam gave smaller values for the frequency than what would be the case for a full floor.

The overall performance of the timber-concrete composite system tested in this thesis was good. However, some adjustments should be made and more research has to be done, if developing this into a new floor system.

v

Sammendrag

Komposittkonstruksjoner i tre og betong ble opprinnelig utviklet for broer og for å forsterke eksisterende tregulv, men er i dag også brukt mye i nye bygninger. Målet med denne oppgaven er å se på de dynamiske egenskapene på en type komposittkonstruksjon hvor betongdekket består av mindre betongelementer limt til hverandre. Skjærforbindelsen brukt i denne oppgaven er et innlimt stålgitter, som har vist høy kapasitet i tidligere studier. Betongen er fiberarmert betong.

En fullskala modell ble bygget i laboratoriet, og følgende tester ble utført: En dynamisk test ("hammer impact test") og en nedbøyningstest med 1 kN last. I tillegg ble det utført en skjærtest på to asymetriske prøvestykker for å finne stivheten til skjærforbindelsen. Den fiberarmerte betongen ble testet separat for å finne materialegenskapene. Det ble i tillegg laget numeriske modeller i ABAQUS for å estimere konstruksjonens oppførsel.

De dynamiske testene viste at komposittkonstruksjonen tilfredsstilte de dynamiske kravene som var satt på forhånd. Gjennom skjærtesten kom det fram at skjærforbindelsen var både svakere og mer duktil enn forventet. Det ble oppdaget at dette skyldtes utilstrekkelig liming under monteringsprosessen. De numeriske analysene ga gode estimater for oppførselen til komposittkonstruksjonen. Det viste seg at stivheten til skjærforbindelsen var mer avgjørende for nedbøyningen av konstruksjonen enn den var for frekvensen. Ved å utvide den numeriske modellen til et gulv i ABAQUS ble det sett at komposittkonstruksjonen muligens gir noe lavere verdier for frekvensen enn det tilfellet ville være for et fullskala gulv.

På et generelt basis viste komposittkonstruksjonen som ble testet å fungere bra i forhold til de krav som ble satt. Det skal likevel presiseres at noen justeringer bør bli gjort og mer forskning må legges ned om det skal utvikles videre til et nytt gulvsystem.

Contents

Notations

Latin upper case letters

A	Area $[mm^2]$
E	Modulus of elasticity $[N/mm^2]$
$E_{0,mean}$	Modulus of elasticity along the grain, glulam $[N/mm^2]$
$E_{90,mean}$	Modulus of elasticity perpendicular to the grain, glulam $[N/mm^2]$
E_p	Modulus of elasticity at specific point $[N/mm^2]$
E_{ref}	Modulus of elasticity of reference material $[N/mm^2]$
$(EI)_0$	Bending stiffness of beam with no composite action $[Nmm^2]$
$(EI)_{ef}$	Efficient bending stiffness $[Nmm^2]$
$(EI)_\infty$	Bending stiffness of beam with full composite action $[Nmm^2]$
$(EI)_{real}$	Actual bending stiffness of composite system, efficiency calculations $[Nmm^2]$
F	Concentrated load $[kN]$
$F(\omega)$	Input signal spectrum
$G_{0,mean}$	Shear modulus, glulam $[N/mm^2]$
$H(\omega)$	Frequency Response Function
I	Second moment of area $[mm^4]$
$I_{y,fic}$	Second moment of area of fictitious cross-section $[mm^4]$
$M_{y,Ed}$	Design value of bending moment $[kNm]$
M	Bending moment $[kNm]$
N	Axial force $[kN]$
Q	Connector force $[kN]$
S	Standard deviation in concrete beam tests
V	Shear force $[kN]$
$X(\omega)$	Output signal spectrum

Latin lower case letters

a	Distance between the neutral axes $[mm]$
b	Width $[mm]$
h	Height $[mm]$
f	frequency $[Hz]$
$f_{c,0}$	Compressive strength along the grain, glulam $[N/mm]$
$f_{c,90}$	Compressive strength perpendicular to the grain, glulam $[N/mm]$
$f_{ct,L}$	Tensile strength, concrete $[N/mm]$
$f_{ft,res,2,5}$	Residual tensile strength, concrete $[N/mm]$
$f_{R,j}$	Residual flexural tensile strength, concrete $[N/mm]$
f_m	Bending strength, glulam $[N/mm]$
$f_{t,0}$	Tensile strength along the grain, glulam $[N/mm]$
$f_{t,90}$	Tensile strength perpendicular to the grain, glulam$[N/mm]$
f_v	Shear strength, glulam $[N/mm]$
k	Slip modulus $[kN/mm]$
l	length $[mm]$
p	Uniformly distributed load in derivation from Kreuzinger $[kN/m]$
q	Uniformly distributed load $[kN/m]$
s	Spacing of shear connectors $[mm]$
u	Shear deformation of the connector $[mm]$
w	Deflection $[mm]$
x	Distance between crack and center in residual tensile strength calculations $[mm]$
z_p	Distance from point of interest to neutral axis $[mm]$

Subscripts

1	Refers in composite calculations to the top layer, i.e. concrete
2	Refers in composite calculations to the bottom layer, i.e. glulam

Greek letters

γ	Shear coefficient
δ	Deflection in concrete beam tests $[mm]$
η	Efficiency of shear connection
ξ	Damping ratio
ρ	Density $[kg/m^3]$
$\sigma_{p,d}$	Stress at specific point in cross-section $[N/mm^2]$
$\tau_{2,max}$	Maximum shear stress in glulam $[N/mm^2]$
ϕ_3	Crack rotation
ω	Radian frequency

Abbreviations

FCA	Full Composite Action
FE	Finite Element
FRF	Frequency Response Function
LOP	Limit Of Proportionality
$LVDT$	Linear Variable Differential Transformer
NCA	No Composite Action
PCA	Partial Composite Action
SLS	Serviceability Limit State
ULS	Ultimate Limit State

1 | Introduction

1.1 Background

Timber-concrete composite structures have been studied for about 70 years. It was originally developed as a strengthening of existing timber structures, but was soon successfully included also in new structures. In USA, McCullough (1943) carried out a study on behalf of the Oregon State Highway Department to look at timber-concrete composite structures in short-span highway bridges. In Europe, timber-concrete composite structures have been mainly used in upgrading existing timber floors in old buildings, but have also been used in new commercial and residential buildings (Ceccotti, 1995). Timber-concrete composite decks are now found in bridges, buildings, piers, wharves, hangar aprons, platforms etc. (Lukaszewska, 2009)

The advantage of timber-concrete composite structures is that the concrete topping will mainly take compression, while the timber takes tension and bending. The connection between them transfers the shear forces which forms between the two elements. Compared to a timber floor this will give a stiffer construction, with increased load capacity and high fire resistance. Compared to a concrete floor the timber-concrete composite floor will be lighter. Problems linked to concrete floors, like cracking in the tensile region, can also be avoided.

Traditionally, the concrete has been cast on top of the timber joists. This is unfortunate as it exposes the timber to a wet environment, making it more prone to e.g. creep. Recent research, by among others Lukaszewska (2009) and Crocetti et al. (2010), in Sweden has looked at the opportunity of using prefabricated concrete slabs. This, along with the choice of shear connector, are both issues that need to be evaluated when designing a timber-concrete composite construction.

1.2 Aims and limitations of the research

The principal objective for this thesis is to investigate the dynamic properties of a timber-concrete composite beam. A novel floor system is used, with prefabricated concrete elements glued to each other with epoxy instead of a continuous concrete slab. The concrete is fibre-reinforced concrete. Several tests will be performed in the laboratory. Primarily a dynamic test, but also a shear test and a deflection test to determine the properties of the shear connector. The results will be compared to numerical analyses done in ABAQUS. It will be investigated how changing the shear stiffness and expanding the model to a full-size floor will affect the frequency. Separate tests will be performed on the fibre reinforced concrete to determine its characteristic values, and is presented in its own chapter.

As the research of this thesis only is going on for 20 weeks the work presented has several limitations. All tests are assuming a simply supported beam, which is not a probable boundary condition in a floor. The long-term effects of the composite beam will not be investigated. Nor will the ultimate strength of the construction. The model presents only a strip of a floor, thus the results obtained will only be relatively representative.

2 | Timber-concrete composite structures

The chapter presents previous research done on timber-concrete composite structures. Studies similar and relevant to the work done in this thesis is emphasized. However, other studies are also included to put the development of timber-concrete composite structures in a historical perspective.

2.1 Early research

The research on timber-concrete composite systems has been ongoing for about 70 years. Some of the first full scale bending tests were performed in the United States in the beginning of the 1940s. At the University of Illinois, Richart and Williams (1943) tested 32 composite beams with different shear connectors in addition to long-term tests of the beams. The shear connectors they tested were steel plates with and without spikes, screws and spikes only and sloped notches with and without spikes. The shear connectors consisting of triangular steel plates and spikes gave the best results, with high load capacity, small slip and deflection, and good composite action. The long-term tests done over a 2 1/2 years period showed little reduction of the strength of the beam due to shrinkage or expansion (Richart and Williams, 1943). Around the same time McCullough (1943) tested 22 beams on behalf of the Oregon State Highway Department, later known as the Oregon tests. The goal was to develop a short-span timber-concrete composite bridge. McCullough looked at five different shear connectors; spikes, daps in the timber, spikes and daps combined, pipe dowels and flat steel plates.

The conclusion drawn from the tests were:

- the ultimate strength for a composite beam is at least twice as for the same elements without any connection.

- the deflection of a composite beam under a given load will be no more than 25% of the corresponding deflection of the same materials used in-

dependently.

- repeated loading did not seem to have any unfavorable effect on the composite beams

In Europe, timber-concrete composite beams have also been successfully used for renovating timber floors in old masonry buildings. The composite floor is rigid enough not only to keep its own shape, but if well connected to the walls, the whole building's shape. This is very favorable in case of earthquakes (Ceccotti, 1995).

2.2 *In-situ* vs. prefabricated

During the years different materials and ways to build timber-concrete composite beams have been tested. Traditionally the systems that have been tested assume the concrete to be cast *in-situ*, on timber beams with mounted shear connectors. This is a so-called "wet" connection. Despite their good performance, there are several drawbacks with this type of systems:

- the introduction of a "wet" component in the "dry" environment typically found in timber buildings

- the time needed for the concrete to cure, meaning the time will pass until the next action can take place on the site.

- the low stiffness and high creep while the concrete cures, meaning propping is necessary to avoid permanent deflections.

- the costs of casting concrete slabs *in-situ*, this includes the cost of transporting fresh concrete and the use of props and formwork.

- the excessive shrinking of concrete, which leads to additional deflection of the beam.

In recent years there has been several studies on timber-concrete composite beams where parts of it or the complete beam has been prefabricated. Lukaszewska (2009) has tested out different timber-concrete composite systems with prefabricated concrete slabs. By prefabricating it is possible to avoid the disadvantages of casting concrete on top of timber. However, using a prefabricated concrete slab requires greater precision when assembling the timber to the concrete, and can be complicated for some types of connections.

Figure 2.1: *Example of an HBV-element and transportation on the construction site (from www.hbv-system.de)*

Bathon et al. (2006) have done extensive research and development of a modular element system called the HBV-system. This system consists of wall-, floor- and roof elements which are connected off site and then transported to the construction site, see figure 2.1. By doing this the issues concerning time and costs in the construction process are avoided. The concrete is though cast directly on the timber, so shrinking of the concrete and exposure of the timber to a wet element are still issues.

In Sweden Crocetti et al. (2010) has looked at the use of fibre reinforced concrete in composite structures. Without the need for steel bar reinforcement it is possible to use thinner elements and by that obtain a more efficient and lighter floor structure.

2.3 Shear connectors

2.3.1 Classification

The shear connectors connecting the timber and concrete is the most important element of a composite structure. The connector should be rigid while under-going stress in the elastic range, but ductile while undergoing stresses in the plastic range (Bathon and Bletz, 2006). Figure 2.2 shows the most commonly used shear connectors as classified by Ceccotti (1995). The shear connectors are divided into four groups according to their stiffness k, also called slip modulus. Connectors in group (a) are relatively inexpensive and easy to install. They are, however, the least rigid and could provide a composite efficiency of under 50%.
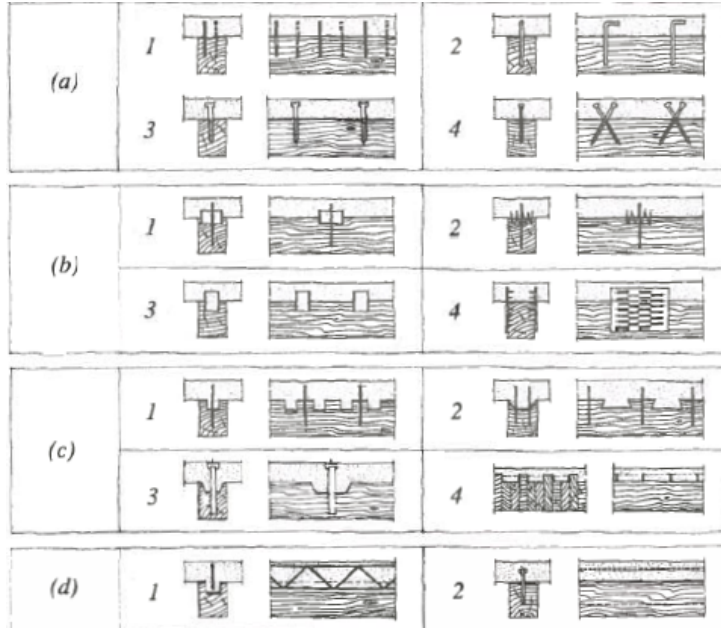
Figure 2.2: *Examples of different shear connectors: (a1) nails; (a2) reinforced concrete steel bars; (a3) screws; (a4) inclined screws; (b1) split rings; (b2) toothed plates; (b3) steel tubes; (b4) steel punched metal plates; (c1) round indentations in timber and fasteners preventing uplift; (c2) square indentations and fasteners; (c3) cup indentations and prestressed steel bars; (c4) nailed timber planks deck and steel shear plates slotted through the deeper planks; (d1) steel lattice glued to timber; (d2) steel plate glued to timber.*

Group (b) connectors are found to have greater stiffness and strength capacity than group (a), while group (c) connectors have similar or better capacity than group (b). Group (d) connectors which consist of glued-in connectors are found to be the most rigid, with a composite efficiency of almost 100% for some types (Ceccotti, 1995; Lukaszewska, 2009).

2.3.2 Adhesives in shear connectors

The use of adhesives has been proven effective both combined with a shear connector or used independently. Compared to mechanical connectors the use of
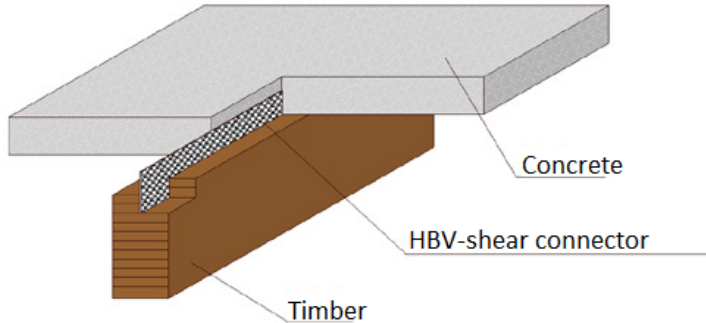
Figure 2.3: *The structural elements of a HBV element (from www.hbv-system.de)*

adhesives such as epoxy glue gives almost no slip between timber and concrete (Lukaszewska 2009, and references therein). However, there are several things to consider when using adhesives in the assembly process, maybe most important the uncertainty around the performance of the adhesive under temperature fluctuations or long-term loading (Clouston et al., 2005). Other aspects is the pot life of the adhesive, i.e. the time it takes from the mixing to the glue is so stiff it cannot be applied. The time the adhesive needs to cure is another issue, as well as the high costs of epoxy resin.

2.3.3 Continuous glued-in connectors

Shear connectors similar to the connector (d2) in figure 2.2 have obtained satisfactory results in several studies. The steel plate is glued into a slot in the timber and the concrete slab is cast on top. A study carried out by Bathon and Graf (2000) looked at the use of a steel mesh connecting the timber beam and the concrete slab. This system was later used for the already mentioned HBV-system, see figure 2.3. The steel mesh was 2x80 mm and reached 40 mm into both timber and concrete. During shear tests failure happened primarily in the wood because of shear. Later studies done with the same connector system used a slip modulus of 415 kN/mm (Bathon and Bletz, 2006).

A similar study done by Clouston et al. (2005) looked at a steel mesh perforated

Figure 2.4: *The steel mesh: (a) in the formwork, (b) prefabricated concrete slab with inserted shear connector (Lukaszewska, 2009)*

and expanded. The mesh was 2x100 mm and reached 50 mm into both timber and concrete. Failure occurred due to rapture of the steel shear connector. The average slip modulus was 415 kN/mm and the effective bending stiffness was 3% less than that of a beam with full composite action (Clouston et al., 2005).

Lukaszewska (2009) tested in her study several shear connectors, among them a steel mesh as shown in figure 2.4. The mesh had a height of 100 mm and reached 50 mm into both timber and concrete. The thickness of the mesh was not stated. The steel mesh provided the highest stiffness among the connectors tested, with a mean slip modulus of 483 kN/mm. Failure occurred in the concrete due to formation of cracks along the steel mesh, followed by rapture of the shear connector. Despite its great stiffness and strength, the steel mesh was excluded from further experimental testing. One of the reasons for this was the accuracy needed when placing the shear connectors in the casting mould. Inaccuracy in this process would cause problems when assembling the concrete slab and the timber beams. Other reasons were the time and cost of the epoxy glue, and it was thereby concluded that the steel mesh was not the easiest shear connector to manufacture (Lukaszewska, 2009).

3 | Composite theory

The chapter gives a brief introduction to the theory behind composite structures. It also includes the calculation method for mechanically jointed beams found in Eurocode 5 (Standard Norge, 2010).

3.1 General

Composite systems include two or more elements connected by a shear transferring connector. In bending the elements tend to slip relative to each other and tangential forces Q are created as the shear connector counteracts the slip. This again leads to the creation of, section by section, axial forces N in opposite direction along the beam length, see figure 3.1. The forces' intensity depend on the stiffness and deformability of the connector. In the case of no connection at all, the axial forces will be zero and the elements will act independently of each other. No shear force is transferred and we get No composite action (NCA), the lower bound of composite action. The higher bound is called Full composite action (FCA), where the connection is infinitely stiff and no slip occur. The axial forces are high and the two materials act like one. Usually, the shear connector generates some slip and we get Partial composite action (PCA). In this case the connector has a finite stiffness. Figure 3.2 presents strain diagrams for structures with no, partial and full composite action.
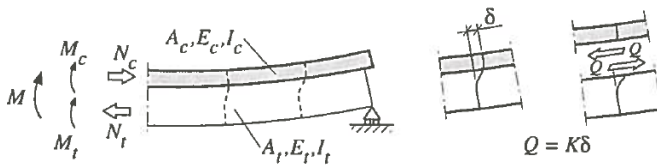

Figure 3.1: *The forces between the elements create compression and bending in the upper layer and tension and bending in the lower layer. From Kreuzinger (1994)*
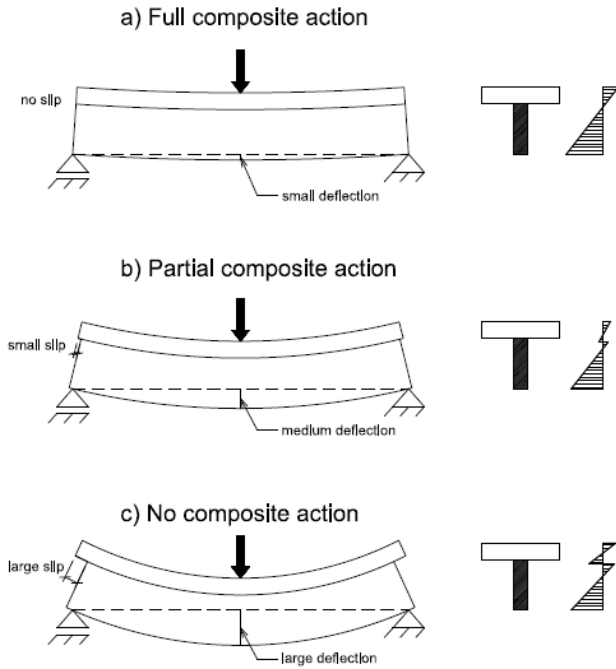
Figure 3.2: *A composite beam in case of a) full composite action, b) partial composite action and c) no composite action*

For a system to be strong and stiff, the shear connector should be efficient. This means the shear forces are effectively transferred through the connector. A way to measure this is using the following equation, originally proposed by Piazza in 1983 (Lukaszewska, 2009):

$$\eta = \frac{(EI)_{real} - (EI)_0}{(EI)_\infty - (EI)_0} \tag{3.1}$$

where η is the efficiency of the connector, $(EI)_\infty$ is the the bending stiffness of the beam with theoretical full composite action, $(EI)_0$ is the bending stiffness of the beam with no composite action and $(EI)_{real}$ is the actual bending stiffness of the beam. When the connection system is very stiff $(EI)_{real}$ is close to $(EI)_\infty$

and thus $\eta \to 1$. If the connection system is very flexible $(EI)_{real}$ is close to $(EI)_0$ and thus $\eta \to 0$.

3.2 Design of composite structures

3.2.1 Full composite action and No composite action

In the case of No composite action and Full composite action the design calculations may be done easily. For NCA the two materials act individually, thus normal bending theory can be used on each element. For FCA there is no slip and the concrete section can be "transformed" into a timber section. This is done by multiplying the width of the concrete with E_c/E_t to acquire the same center of gravity. The stresses throughout the cross-section can then be found from the following equation:

$$\sigma_{p,d} = \frac{E_p}{E_{ref}} \frac{M_{y,Ed}}{I_{y,fic}} |z_p| \tag{3.2}$$

where $\sigma_{p,d}$ and E_p is the stress and the modulus of elasticity at the point of interest, respectively. z_p is the distance from the point of interest to the neutral axis, while E_{ref} is the modulus of elasticity of the reference material (in this case the timber) and $I_{y,fic}$ is the area moment of inertia of the fictitious cross-section.

3.2.2 Partial composite action

In the case of Partial composite action the bending theory does not apply because of the slip between the materials. To find the stress distribution differential equations of equilibrium have to be used. Below is a condensed version of the procedure found in Kreuzinger (1994). It is meant to provide some background knowledge to understand the equations used in the calculations of timber-concrete composite structures. The method has proved to give very good approximations for beams with closely spaced fasteners (Lukaszewska, 2009).

Figure 3.3 shows the deformations of a composite beam in bending where u_1 and u_2 are the longitudinal displacement of the neutral axis of the two elements. w is the bending deflection and u is the shear deformation of the core or the connector system. a is the distance between the neutral axis of the two elements, i.e. $a = h_1/2 + h_2/2$. With simple bending theory one gets the following
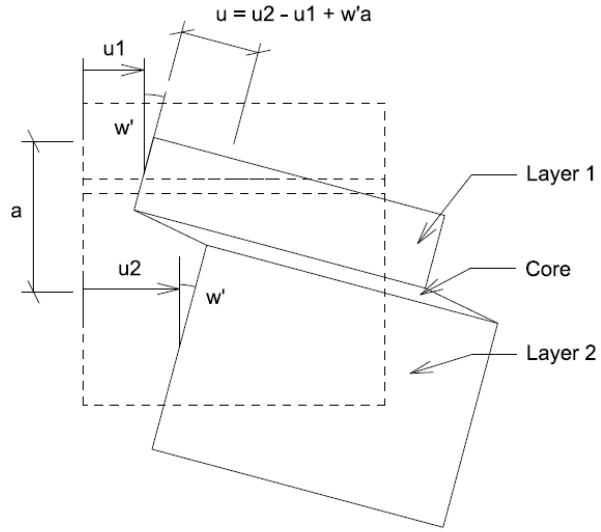
Figure 3.3: *The original and displaced configuration*

equations:

$$N_i = E_i A_i u_i' \tag{3.3}$$

$$M_i = -E_i I_i w'' \tag{3.4}$$

$$V_i = -E_i I_i w''' \tag{3.5}$$

$$Q = ku = k(u_2 - u_1 + w'a) \tag{3.6}$$

Equilibrium in x- and z-direction gives:

$$N_1' + Q = 0 \tag{3.7}$$

$$N_2' + Q = 0 \tag{3.8}$$

$$M_1' = V_1 - Q\frac{h_1}{2} \tag{3.9}$$

$$M_2' = V_2 - Q\frac{h_2}{2} \tag{3.10}$$

By differentiating the sum of Eq. 3.9 and 3.10 and replacing $(V_1' + V_2')$ with the term -p:

$$M_1'' + M_2'' + Q'a + p = 0 \tag{3.11}$$

Then the internal forces and moments can be replaced with the elasticity principles, and the following set of differential equations are obtained:

$$E_1 A_1 u_1'' + k(u_2 - u_1 + w'a) = 0 \tag{3.12}$$

$$E_2 A_2 u_2'' - k(u_2 - u_1 + w'a) = 0 \tag{3.13}$$

$$(E_1 I_1 + E_2 I_2)w'''' - k(u_2' - u_1' + w''a)a = p \tag{3.14}$$

A simple solution can be given for single span beams with a sinusoidal load distribution, because the shape of the deformations in the direction of the axes also correspond to sin- or cos-functions. Although the solution is acquired from a sinusoidal load distribution it is applied successfully to many other types of load distributions. Given:

$$p = p_0 sin\left(\frac{\pi}{l}x\right) \tag{3.15}$$

the deformations will be

$$u_1 = u_{10}cos\left(\frac{\pi}{l}x\right); \quad u_2 = u_{20}cos\left(\frac{\pi}{l}x\right); \quad w = w_0 sin\left(\frac{\pi}{l}x\right) \tag{3.16}$$

where u_1, u_2 and w are determined by solving the system of equations 3.12-3.14. This gives the solution:

$$w_0 = p\frac{l^4}{\pi^4}\frac{1}{E_1 I_1 + E_2 I_2 + \dfrac{E_1 A_1 \gamma_1 a^2}{1 + \gamma_1 \dfrac{E_1 A_1}{E_2 A_2}}} = p_0\frac{l^4}{\pi^4}\frac{1}{(EI)_{ef}} \tag{3.17a}$$

$$u_{10} = w_0\frac{\pi}{l}\frac{a\gamma_1 E_2 A_2}{\gamma_1 E_1 A_1 + E_2 A_2}; \tag{3.17b}$$

$$u_{20} = -w_0\frac{\pi}{l}\frac{a\gamma_1 E_1 A_1}{\gamma_1 E_1 A_1 + E_2 A_2} \tag{3.17c}$$

where $\quad \gamma_1 = \dfrac{1}{(1 + k_1)} \quad$ and $\quad k_1 = \dfrac{\pi^2}{l^2}\dfrac{E_1 A_1}{k}$

Stresses in the cross-section can be found based on these deformations and by applying elastic principles. For example, the stress in the axis of part 1 is:

$$\sigma_1 = E_1 u_1'(x = l/2) = -E_1 u_{10}\frac{\pi}{l} \tag{3.18}$$

Using the following terms:

$$w_0 = p_0\frac{l^4}{\pi^4}\frac{1}{EI_{ef}}; \qquad\qquad\qquad M_0 = p_0\frac{l^2}{\pi^2}$$

$$a_2 = \frac{\gamma_1 E_1 A_1 a}{\gamma_1 E_1 A_1 + E_2 A_2}; \qquad\qquad\qquad a_1 = a - a_2$$

the stress is

$$\sigma_1 = \frac{\gamma_1 E_1 a_1 M_0}{(EI)_{ef}} \tag{3.20}$$

The procedure derived here presents the basis behind the equations found in Eurocode 5 Annex B "Mechanically jointed beams", which is presented in the next section.
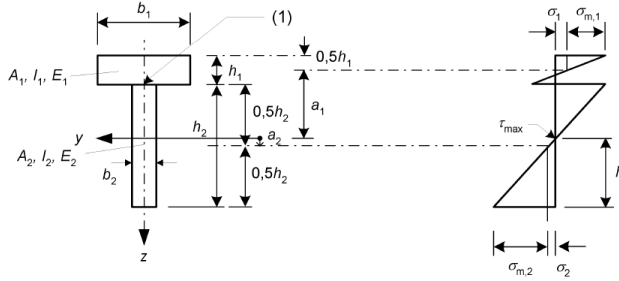
Figure 3.4: *Cross-section (left) and stress distribution (right) of a composite beam with partial composite action (from Eurocode 5)*

3.2.3 The γ-method

Eurocode 5 - Part 1-1, Annex B provides a simple method for calculating stresses in the component materials and maximum deflection for mechanically jointed beams. The equations are based on linear elasticity theory and derived above. Eurocode 5 states the following assumptions:

- The beam is simply supported with a span L. For continuous beams the expressions can be used with L equal to 0.8 times the actual span, and for cantilevered beams L is equal to twice the length of the cantilever.

- The individual parts (of wood or wood-based panels) are either in full length or made with glued end joints.

- The individual parts are connected to each other by mechanical fasteners with a slip modulus k.

- The distance s between the fasteners is constant or varies uniformly according to the shear force between s_{min} and s_{max}, with $s_{max} \leq 4s_{min}$.

- The load acts in the z-direction, creating a moment $M = M(x)$ which varies sinusoidally or parabolically, and a shear force $V = V(x)$.

15

The effective bending stiffness $(EI)_{ef}$ of a two element composite beam is given as:

$$(EI)_{ef} = \sum_{i=1}^{2}(E_i I_i + \gamma_i E_i A_i a_i^2) \tag{3.21}$$

where E_i, I_i and A_i are the modulus of elasticity, the second moment of area and the area of the two composite materials respectively. The shear coefficients γ_i and distances a_i are given as:

$$\gamma_1 = \left[1,0 + \frac{\pi^2 E_1 A_1 s_1}{k_1 l^2}\right]^{-1} \tag{3.22}$$

$$\gamma_2 = 1,0 \tag{3.23}$$

$$a_1 = \frac{h_1 + h_2}{2} - a_2 \tag{3.24}$$

$$a_2 = \frac{\gamma_1 E_1 A_1 (h_1 + h_2)}{2 \sum_{i=1}^{2} \gamma_i E_i A_i} \tag{3.25}$$

where s_i is the connector spacing, k_i the slip modulus of the shear connector and l is the beam length. Remaining variables are found in figure 3.4.

The effective bending stiffness is used to calculate the stress distribution, the load on the fastener and the deflection. The following equations are applied for a simply supported beam with uniform load:

16

$$\sigma_i = \frac{\gamma_i E_i a_i M}{(EI)_{ef}} \tag{3.26}$$

$$\sigma_{m,i} = \frac{0,5 E_i h_i M}{(EI)_{ef}} \tag{3.27}$$

$$\tau_{2,max} = \frac{0,5 E_2 h_2^2 V}{(EI)_{ef}} \tag{3.28}$$

$$F = \frac{\gamma_1 E_1 A_1 a_1 s_1 V}{(EI)_{ef}} \tag{3.29}$$

$$w = \frac{5ql^4}{384(EI)_{ef}} \tag{3.30}$$

where σ_i and $\sigma_{m,i}$ are the normal stresses, $\tau_{2,max}$ is the maximum shear stress, F is the load on the fastener, w is the mid-span deflection, M is the bending moment and V is the shear force in the cross-section of interest.

3.2.4 Slip modulus

The load-slip relationship of the shear connector is non-linear, which makes it necessary to operate with several slip moduli. Ceccotti (1995) proposed two different values; k_{ser} for the serviceability limit state (SLS) and k_u for the ultimate limit state (ULS). k_{ser} is taken as the secant value at 40% of the load-carrying capacity, while k_u is taken as the secant value at 60%. In general, the values of the slip moduli should be determined by tests according to EN 26891 (Standard Norge, 1991). However, if there is no experimental data available, Eurocode 5 Part 1-1 proposes using the formulas for k_{ser} in timber-to-timber connections and multiply the value by 2. k_u is then taken as 2/3 of k_{ser}, also according to Eurocode 5. This method is convenient depending on the type of connector. Ceccotti et al. (2007) found the analytical results based on Eurocode 5 to largely underestimate both strength and stiffness of the connector tested, with a difference up to 50% between the analytical and experimental values of the slip moduli.

4 | Materials and method

This chapter presents the concept and construction of the timber-concrete composite beam tested in this thesis. Specifications of the materials are given, as well as a detailed description of the assembly of the beam. The chapter also includes a presentation of the test program and the numerical models used for comparison.

4.1 Materials

4.1.1 Glulam

The joists are made of glue laminated members in the Nordic strength class CE L40C, which has recently replaced GL32C. The strength and behaviour are approximately equivalent (Lukaszewska, 2009). The material parameters are presented in table 4.1 (Moelven, 2012).

Bending	$f_{m,k}$	30.8 N/mm^2
Tension	$f_{t,0,k}$	17.6 N/mm^2
	$f_{t,90,k}$	0.4 N/mm^2
Compression	$f_{c,0,k}$	25.4 N/mm^2
	$f_{c,90,k}$	2.7 N/mm^2
Shear	$f_{v,k}$	3.5 N/mm^2
Modulus of elasticity	$E_{0,mean}$	13000 N/mm^2
	$E_{0,05}$	10500 N/mm^2
	$E_{90,mean}$	410 N/mm^2
Shear modulus	$G_{0,mean}$	760 N/mm^2
Density	ρ_k	400 kg/m^3
	ρ_{mean}	470 kg/m^3

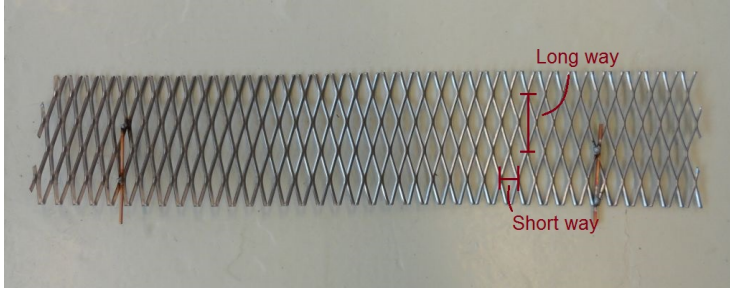Table 4.1: *Properties of CE L40C*

18

Figure 4.1: *The expanded metal. The sticks welded to the lower part are to maintain a gap between the mesh and the surface of the concrete. The long and short way are marked on the figure.*

4.1.2 Fibre reinforced concrete

The concrete used for the composite beam is classified B30, reinforced with steel fibres with a density of 40 kg/m^3. The fibres are 40 mm long with a hooked end. To reduce shrinkage the mixture Mapecure SRA was added, in addition to a superplasticizer to reduce water in the concrete. The strength properties of the concrete was tested and is described in chapter 5. When dimensioning the beam, properties for B30 concrete from Eurocode 2 (Standard Norge, 2008b) was assumed. In the numerical analyses a modulus of elasticity $E = 30000$ N/mm^2 and a density of $\rho = 2400$ kg/m^3 are used.

4.1.3 Steel mesh

As a shear connector a steel mesh was chosen. Similar connectors has been used in previous studies showing a high grade of composite action. The mesh used as a shear connector in this thesis is an expanded metal, see fig 4.1, of type S235 steel. The long way of the mesh is 38 mm and the short way 12 mm. The strand width and thickness is 3,1 mm and 1,6 mm, respectively. The thickness of the steel mesh itself varies, but is taken as approximately 3 mm.

4.1.4 Epoxy

The adhesive used to connect the steel mesh to the timber and the concrete slabs to each other is a two component fast curing epoxy glue, Mapepoxy L.

Technical specifications are found in the table 4.2 (Mapei, 2012). The numbers are based on a curing temperature of 20° C and a curing time of 7 days. The opening time of the glue is from the producer sat as 1 hour. The epoxy glue is initially meant as a cohesion between concrete or between concrete and steel, but was recommended also for the cohesion between timber and steel.

Compressive strength	110 N/mm^2
Tensile strength	20 N/mm^2
Flexural tensile strength	40 N/mm^2
Modulus of elasticity	17500 N/mm^2
Density	2.0 g/cm^3

Table 4.2: *Properties of the epoxy glue*

4.2 Construction of the composite beam

The type of timber-concrete composite system tested in this thesis consists of several fibre reinforced concrete slabs with a steel mesh imbedded. The steel mesh, which works as a shear connector, is glued into a slot in a glulam joist with an epoxy adhesive. The concrete slabs are glued to each other to obtain a continuous stress distribution along the beam, also with an epoxy adhesive.

A full-scale model of a composite floor strip was constructed with two glulam joists in center distance 600 mm and a concrete deck. The floor strip is from here referred to as the composite beam. In addition, two asymmetrical specimens were made for the shear test. The beam was dimensioned so it would fulfill the requirements of the respective Eurocodes (Standard Norge). It was intended a 8 m span, which is usually found in commercial buildings. It was therefore assumed a design load in the category of congregational area from Eurocode 1 (Standard Norge, 2008a). The glulam joists were designed for service class 1 in Eurocode 5. Since there was no knowledge of the stiffness of the shear connector a stiffness of k = 415 kN/mm was assumed in the Serviceability Limit State (SLS), based on previous research. To ensure a frequency above the critical limit of 8 Hz defined by Eurocode 5, a frequency criteria originally proposed by Hu and Chui (2004) was used:

$$w < (\frac{f}{18.7})^{2.27} mm \qquad (4.1)$$
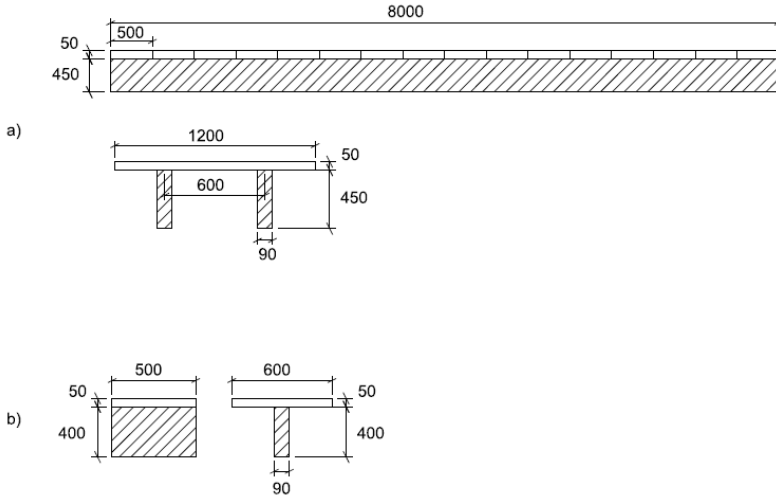
Figure 4.2: *The full-scale beam above (a) and the shear test specimen underneath (b)*

where w is the deflection from 1 kN load and f is the fundamental frequency in Hz. Eq. 4.1 is based on people's perception of vibrations in correlation to deflection and natural frequency. For a simply supported beam the deflection and frequency can be written like this:

$$w = \frac{Fl^3}{48EI} \quad \text{and} \quad f = \frac{\omega}{2\pi} = \frac{\pi^2 \sqrt{\dfrac{EI}{ml^4}}}{2\pi} \tag{4.2}$$

The dimensions of the two models can be seen in fig 4.2. Details on the dimensioning are found in the appendix.

The casting of the concrete took place March 18th 2013 at the Materials Technology Laboratory at NTNU. 19 concrete elements 1200 x 50 x 500 mm^3 were made, where 16 were for the full-scale model, 2 for the shear test models and one for testing of the concrete properties. In addition six cylinders and one standard beam were cast at the same time as the elements, also for testing of the concrete properties. The steel mesh was cut in sections of 100 x 500 mm^2.

21
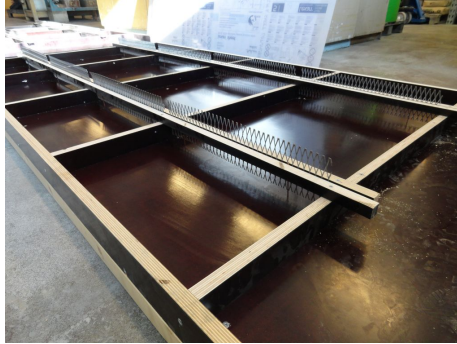
Figure 4.3: *The steel mesh placed in the formwork*

(a)   (b)

Figure 4.4: *Cracking in the concrete slabs (a) right after removing formwork and (b) when mounting the slabs to the glulam*

Two metal sticks were welded to the steel meshes to obtain a cover of 10 mm to the concrete surface, as seen in fig 4.1. The steel meshes were then placed in the formwork so 40 mm would be embedded into the concrete and the remaining 60 mm glued to the glulam beam. There were two steel meshes in every element, with a center distance of 600 mm. Fig 4.3 shows the set-up of the steel mesh in the formwork. The formwork was removed two days after casting, and the concrete slabs put aside to cure for 28 days. When moving the concrete slabs a weak area was discovered around the embedded steel mesh, when one concrete slab cracked in this area due to lifting in the short ends. Fig 4.4a shows the failure pattern.

Figure 4.5: *The slot routed in the glulam*

The 16 concrete elements were all connected to two 90 x 450 x 8500 mm^3 glulam joists to make the full-scale model. It was left 250 mm on each side of the joists without any concrete deck. To mount the concrete elements to the glulam beams, a 6 mm wide and 65 mm deep slot was routed in the members, see fig 4.5. The slot was filled to half its depth with epoxy before inserting the embedded steel meshes into the slot. For the full-scale model, the epoxy was also poured in between the concrete elements to glue them together. Protection was placed underneath the joints to prevent the epoxy of leaking through. The composite beam was placed on a small bulged molding on each side, so it could be assumed as simply supported. The span between the supports were 8 m. The finished composite beam can bee seen in figure 4.6.

One problem occurred during the assembling of the full-scale model. When mounting the concrete elements to the glulam joists, some elements were pounded with a hammer to place them as close as possible to the next element. This caused two elements to crack on the surface, in the area where the shear connector was placed, see fig 4.4b. This supported the suspicion of the area around the steel mesh being weaker than the rest of the concrete element. However, it was assumed it would not affect the overall performance of the beam.

As one element cracked when the formwork was removed, there was only one element left for the shear test specimens. This element was sawn in two (600 x 50 x 500 mm^3) and each part was connected to a 90 x 400 x 500 mm^3 glulam member. The assembly was like explained for the composite beam. The shear

Figure 4.6: *The composite beam*

Figure 4.7: *The shear test specimen*

test specimen is shown in figure 4.7.

4.3   Shear test

A shear test was performed to determine the load-displacement relationship and the slip modulus of the shear connector. Two different asymmetrical specimens were tested. Each consisted of a 600 x 50 x 500 mm^3 concrete slab connected to a 90 x 400 x 500 mm^3 glulam member. Figure 4.8 shows the test set-up. The specimen is placed with the concrete slab on a support. The timber is only supported on the side to a steel beam with a sheet of Teflon placed between the steel and the timber to minimize friction. Load was applied according to EN
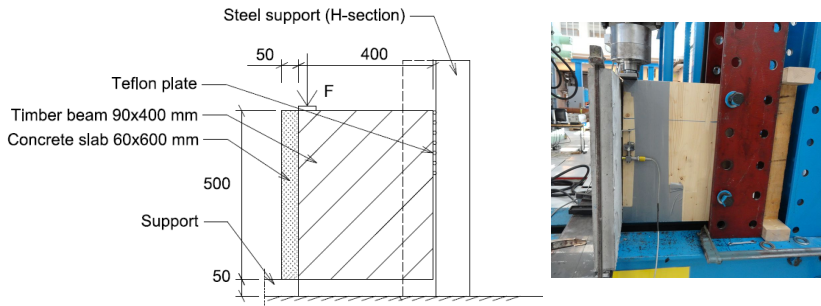
Figure 4.8: *Set-up of the shear test*

(a)   (b)

Figure 4.9: *The modal hammer (a), and the accelerometer (b)*

26891, using a 100 kN hydraulic jack. Data was recorded with a frequency of 5 Hz, i.e. every 0.2 s. Two Linear Variable Differential Transformers (LVDT) were placed on each side of the glulam element to measure the relative slip between the concrete slab and the glulam element.

A disadvantage of the asymmetrical shear test is a slightly overestimation of the shear strength. This is due to the eccentricity of the axial force which creates an overturning moment. This again, will result in a compression force between the timber and concrete and thus increase the friction between them (Lukaszewska, 2009). It therefore has to be assumed that the slip modulus derived from this test is higher than the actual slip modulus.

4.4   Dynamic test

A dynamic test was performed on the full-scale model. To measure the dynamic properties of the structure a hammer test was used. This is a quick and easy way to find eigenfrequencies and damping. It requires a modal hammer (fig 4.9a) and an accelerometer (fig 4.9b). By hitting the structure with the hammer, a wide frequency range is initiated. The method used for this test is called the roving hammer method. It involves placing the accelerometer at one spot, and then apply the hammer force on several points along the beam. The data is recorded and processed via the analytical software LabVIEW. The modal parameters frequency, damping and mode shapes are obtained from a Frequency Response Function (FRF). The FRF $H(\omega)$ has the following relationship to the input signal spectrum from the hammer $F(\omega)$ and the output signal spectrum from the accelerometer $X(\omega)$:

$$H(\omega) = \frac{X(\omega)}{F(\omega)} \tag{4.3}$$

There is one FRF created for every hammer point, which together form a matrix $H_{i,j}$. The signals were curve fitted to fit the following expression:

$$H_{i,j} = \sum_{r=1}^{n} \frac{(\psi_i \psi_j)_r}{[\omega_r^2 - \omega^2 + 2j\xi_r \omega_r \omega]} \tag{4.4}$$

where $(\psi_i \psi_j)_r$ are the residues, ω_r is the modal frequency, ξ_r is the modal damping ratio, r is the mode number and n the total number of nodes. For the test carried out in this thesis 30 hammer points were used. 3 along the width of the beam (i=3), placed 300 mm apart, and 10 along the length of the beam (j=10), placed 800 mm apart. The outermost rows of points are placed above the glulam joists, see fig 4.10. Three tests were performed, where the accelerometer was placed on each of the glulam joists and in the middle of the concrete span, respectively. The glulam joists are from here referred to as Beam N and Beam S, where Beam N is the joist placed towards north and Beam S the joist placed towards south. The accelerometer was placed 660 mm from center of the span to avoid being where one of the mode shape's amplitude was zero.
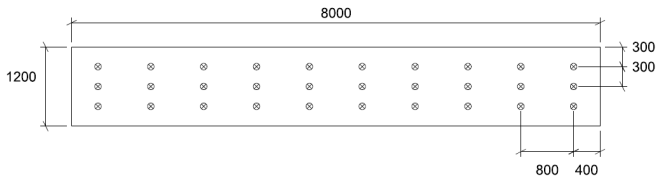
Figure 4.10: *Placing of the points for hammer testing along the concrete deck*
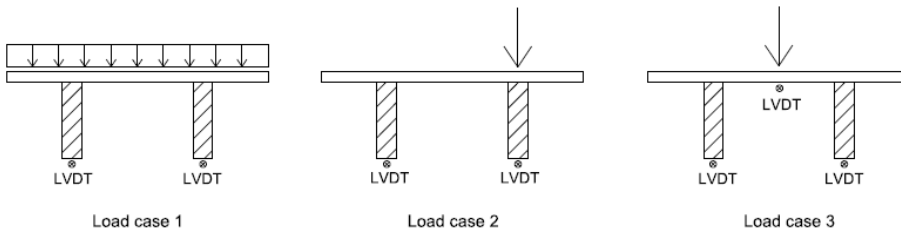
Figure 4.11: *The three load cases with placements of the LVDTs*

Figure 4.12: *The weights applied in load case 3*

4.5   Deflection test

A 1 kN load was applied in different load cases at the full-scale beam to measure the deflection at mid-span. Three load cases were examined, see fig 4.11: Load case 1 where the load is uniformly distributed along the width of the beam with a spreader. Load case 2 where the load is placed upon Beam N. And load case 3 where the load was placed in the middle of the concrete span. The load was applied mid-span of the composite beam in all load cases. The load consisted of two weights with a mass of 50.0 kg and 50.1 kg, which comes to 0,982 kN. Figure 4.12 shows the appearance of the weights. Two LVDTs were placed underneath each of the glulam joists to measure the deflection, and a third LVDT was placed underneath mid-span of the concrete for load case 3.

4.6   Numerical analysis

Three finite element (FE) models were created in ABAQUS to examine the performance of the timber-concrete composite system. ABAQUS is a popular computer software for finite element analysis. The first model illustrates the shear test and was used to estimate the stiffness of the shear connection. The second model illustrates the full-scale beam and was used to look at vibrations and deflection of the system. The third was an extension of the full-scale beam to a whole floor to see how that would affect the dynamic properties.
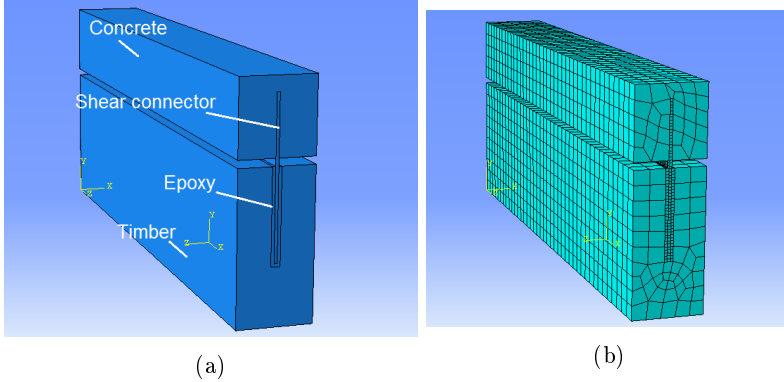
Figure 4.13: *FE model for shear testing (a) and mesh (b)*

4.6.1 FE model for shear testing

The model used for shear testing consists of a timber beam (50 x 50 x 400 mm^3) with a 6 mm wide and 62 mm deep slot. The slot contains a 2 mm thick layer of epoxy along all sides and then a 2 mm wide material imitating the steel mesh. The shear material is embedded in a concrete beam (50 x 50 x 400 mm^3). Figure 4.13a shows the FE model. C3D8, 8 node linear brick elements, were used for all parts.

All materials were modelled as elastic materials. The glulam was in addition modelled as a transversely isotropic material to resemble the difference between behaviour parallel to grain and normal to grain. In order for ABAQUS to model a non-isotropic material the engineering constants have to be transformed into stiffness parameters. The procedure for doing this is taken from Daniel and Ishai (2006) and the calculations can be found in the appendix. The parameters used for the materials are the ones listed in section 4.1

The aim for the shear test model was to get an indication of what would be the weakest element of the shear connection. It was also to imitate the deformations found in the shear test by changing the modulus of elasticity of the shear material.
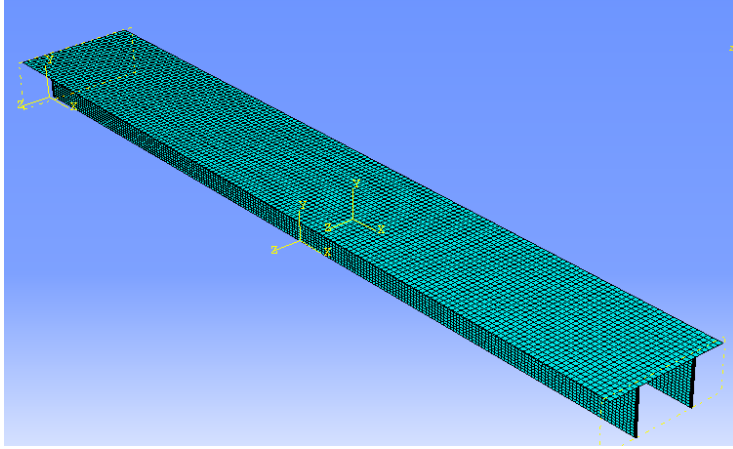
Figure 4.14: *FE model for dynamic testing*

4.6.2 Full scale FE model

The model of the full scale beam consists 16 concrete slabs (1200 x 50 x 500 mm^3) on top of two timber joists (90 x 450 x 8000 mm^3). The concrete slabs were connected to the joists by a 5 x 5 x 8000 mm^3 shear material simplifying the real connection with a steel mesh and epoxy glue. The shear material was given the same properties as the shear material in the shear test FE model. The epoxy layer between the concrete elements were ignored, as analyses done in a smaller scale showed it would have little effect on the frequencies. The full-scale FE model can be seen in fig 4.14. As in the shear test FE model all materials were elastic and the timber transversely isotropic. S4, 4 node shell elements, were used for all parts. A refined mesh was made near the supports to avoid large deformations in the elements.

A frequency analysis was performed and compared to the frequencies found from the dynamic impact test. A general static analysis was performed with the three load cases from section 4.5, and deflections were compared with the ones found in the deflection test.
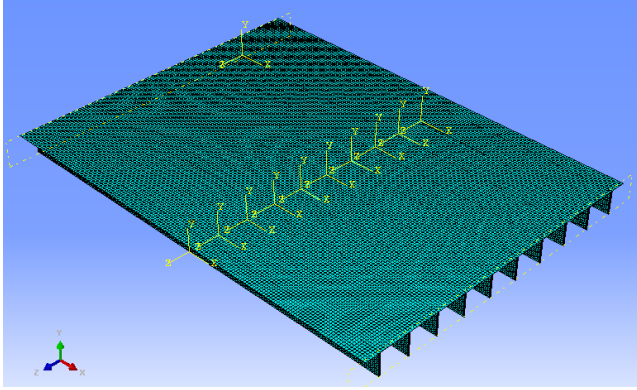
Figure 4.15: *FE model of floor*

4.6.3 FE model of floor

The full-scale beam model was extended to a 6 m wide floor with 10 glulam joists, still with a span length of 8 m and a center distance between the joists of 600 mm. It was used a continuous concrete slab to simplify the model. The glulam joists in the floor was simply supported, while the free ends of the concrete were constrained to move in the y-direction. Figure 4.15 shows the FE model of the floor. A frequency analysis was carried out and compared to the results from the testing of the full-scale beam.

5 | Fibre reinforced concrete. Testing and results of standard beams

6 cylinders, 1 standard beam and 3 plates were cast at the same time as the concrete elements. Tests were done to determine the flexural tensile strength and the compressive strength of the concrete. The set-up of the tests and results are presented in this chapter, together with an evaluation of the test results compared to theoretical values.

5.1 Fibre reinforced concrete

Concrete has a low tensile strength, and is in most cases in need of reinforcement to take the tensile forces when the concrete cracks. Fibres present an option to conventional reinforcement in cases where only minimal reinforcement is required, or as a supplement to conventional reinforcement. Adding fibres increases the residual strength of the structure (Sandbakk, 2011).

5.2 Method

5.2.1 Cylinder test

Six cylinders were cast at the same time as the concrete elements. A compressive strength test was performed to determine the compressive strength of the fibre reinforced concrete. Dimensions of the cylinders and testing procedures were in accordance with the NS-EN 12390 series (Standard Norge, 2005). All specimens were approximately 100 mm in diameter and 200 mm in height. They were loaded with a compression force until failure. In addition the cylinders were weighed both in air and water to find the weight and volume. The results from this is found in the appendix.
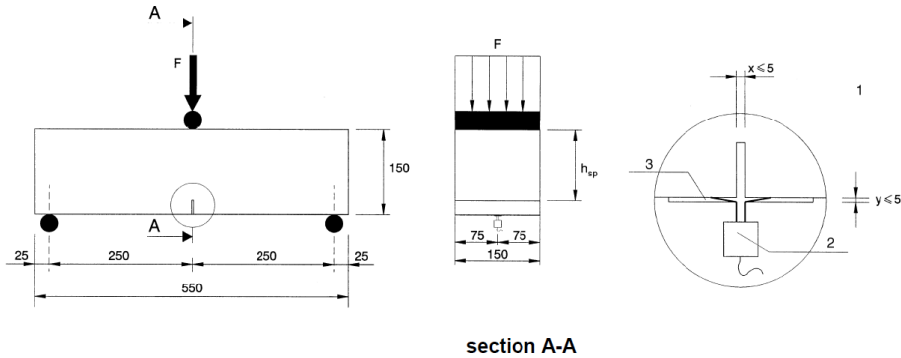
Figure 5.1: *Set-up for standard beam (from NS-EN 14651)*

5.2.2 Beam test

One standard beam and one concrete element (50 x 500 x 1200 mm^3) were cast at the same time as the concrete elements. Beam tests were performed to find the residual tensile strength of the fibre reinforced concrete. The standard beam was tested in accordance with NS-EN 14651 (Standard Norge, 2012). The concrete element was sawn into three plates (50 x 150 x 550 mm^3) and tested in accordance with Norwegian Sawn Beam Test (NSBT). The two tests are described below.

NS-EN 14651

The set-up for testing the standard beam was as described in NS-EN 14651. A 5 mm notch was sawn in the beam and a center load was applied mid-span distributed over the whole width of the specimen. Fig 5.1 shows the set-up. A LVDT was placed on each side of the specimen to measure the deflection. To find the residual flexural tensile strength the Crack Mouth Opening Displacement (CMOD) is needed. This is found through the relationship:

$$\delta = 0.85 CMOD + 0.04 \tag{5.1}$$

where δ is the deflection. The residual flexural tensile strength is then:
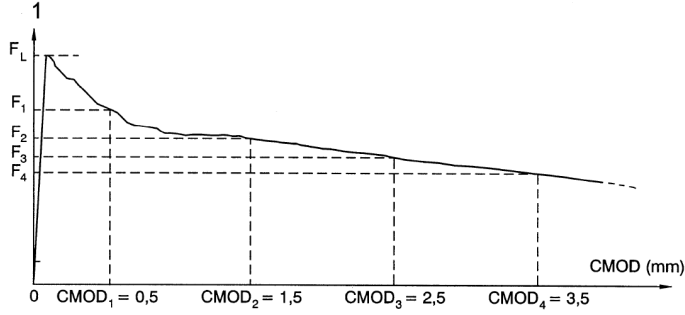
Figure 5.2: *The load-CMOD diagram (from NS-EN 14651)*

$$f_{R,j} = \frac{3F_j l}{2bh_{sp}^2} \tag{5.2}$$

where $f_{R,j}$ is the residual flexural tensile strength and F_j the load corresponding with $CMOD = CMOD_j$. l is the span length, b the width of the specimen and h_{sp} is the distance between the tip of the notch and the top of the specimen. Figure 5.2 shows the relationship between $CMOD_j$ and F_j. Characteristic residual flexural tensile strength is then taken as

$$f_{Rk,j} = f_{R,j} - kS \tag{5.3}$$

where S is the standard deviation of the test series and $k = 1.7$ when the test set-up is as described in NS-EN 14651. The characteristic residual tensile strength $f_{ftk,res,2,5}$ is calculated from the characteristic residual flexural tensile strength at 2.5 mm crack width:

$$f_{ftk,res,2,5} = 0.37 f_{Rk,3} \tag{5.4}$$

The limit of proportionality (LOP) can be found by the following expression:

$$f_{ct,L}^f = \frac{3F_L l}{2bh_{sp}^2} \tag{5.5}$$

34

(a)   (b)
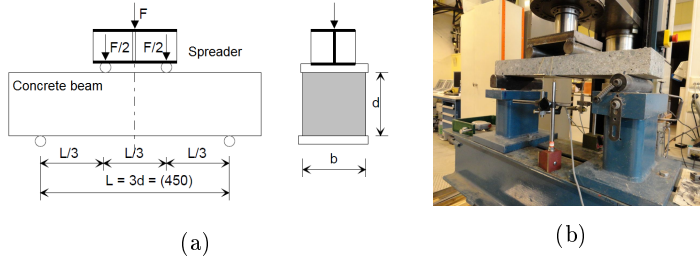
Figure 5.3: *The NSBT. The set-up (Kanstad, 2011) (a), and picture of testing (b)*
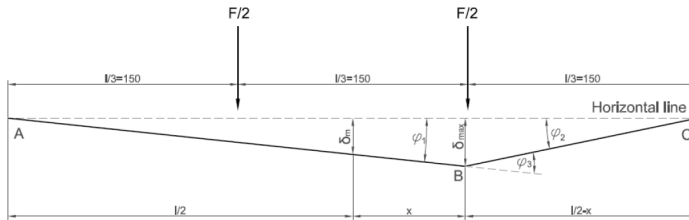
Figure 5.4: *Crack offset for the NSBT method (Sandbakk, 2011)*

where F_L is the load corresponding to the LOP. It is the highest load value within the first 0.05 mm. The LOP is defined as the stress at the tip of the notch.

Norwegian Sawn Beam Test

For the plates, a Norwegian Sawn Beam Test (NSBT) was performed instead of the beam test from NS-EN 14651. This was due to the fact that the plates were sawn and were relatively thin. The NSBT is carried out as a four-point test with two loads distributed over the whole width of the specimen. See figure 5.3 for the set-up. There is no notch sawn in the plates. This means the crack in the specimen will most likely occur other places than at mid-span. It is therefore necessary to look at the crack offset and calculate the crack rotations. The following procedure is from Sandbakk (2011) and shows how to derive CMOD with crack offset:
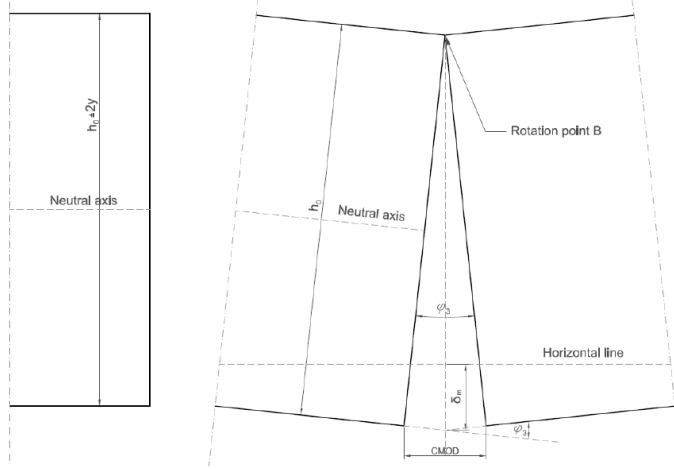
Figure 5.5: *Relationship between CMOD, δ and φ₃ (Sandbakk, 2011)*

$$\phi_1 = \frac{2\delta_m}{l} = \frac{2\delta_{max}}{l+2x} \Rightarrow \delta_{max} = \frac{\delta_m(l+2x)}{l} \tag{5.6}$$

$$\phi_2 = \frac{2\delta_{max}}{l-2x} = \frac{2\delta_m(l+2x)}{l(l-2x)} \tag{5.7}$$

$$\phi_3 = \phi_1 + \phi_2 = \frac{4\delta_m}{l-2x} \tag{5.8}$$

where ϕ_j are the crack rotations, δ_m is the measured deflection, δ_{max} is the deflection at the crack and x is the crack offset, as seen in fig 5.4. Figure 5.5 shows the relationship between ϕ_3, δ and *CMOD*. This can be expressed as:

$$CMOD = (h_0 \pm 2y)\phi_3 = 4\frac{h_0 \pm 2y}{l-2x}\delta_m \tag{5.9}$$

where h_0 is the prescribed height of the beam, $\pm 2y$ is the deviation from the prescribed h_0 and δ_m the measured deflection. By knowing the CMOD the residual flexural tensile strength can be found by following the procedure for NS-EN 14651.

36

Specimen	Maximum load at failure F_{max} [kN]	Compressive strength f_{ck} [N/mm^2]
Cylinder 1	314.22	40.82
Cylinder 2	315.91	41.04
Cylinder 3	312.74	40.63
Cylinder 4	323.18	41.98
Cylinder 5	295.79	39.21
Cylinder 6	327.47	42.54
Average	**314.89**	**41.04**

Table 5.1: *Results from cylinder testing*

5.3 Results

5.3.1 Cylinder test

Tests were carried out in the Materials Technology Laboratory at NTNU May 13th 2013, 56 days after casting. The cylinders were tested with a loading rate of 0.5 N/mm^{2}s. Table 5.1 shows the compressive strengths f_{ck} and maximum load at failure F_{max} for the six specimens. Average compressive strength is 41.04 N/mm^2.

5.3.2 Beam test

Tests were carried out in the Materials Technology Laboratory at NTNU April 24th (for the beam) and May 6th 2013 (for the plates) 37 and 49 days after casting, respectively. Dimensions of the beam and plates are found in the appendix.

Plots of the flexural tensile stress-CMOD relationship are shown in figure 5.6 and 5.7. The flexural tensile strength $f_{R,3}$ at $CMOD_3 = 2.5$ mm is the value of interest to find the residual tensile strength $f_{ftk,res,2,5}$. Flexural tensile strengths at relevant CMODs are shown in table 5.2. It was chosen not to use characteristic flexural tensile strength to calculate the residual tensile strength due to the big deviation in the test results and the low number of specimens. The average residual flexural tensile strength $f_{R,3}$ was found to be 2.13 N/mm^2 and the average residual tensile strength $f_{ftk,res,2,5}$ of 0.789 N/mm^2. Average values are for the plates only.
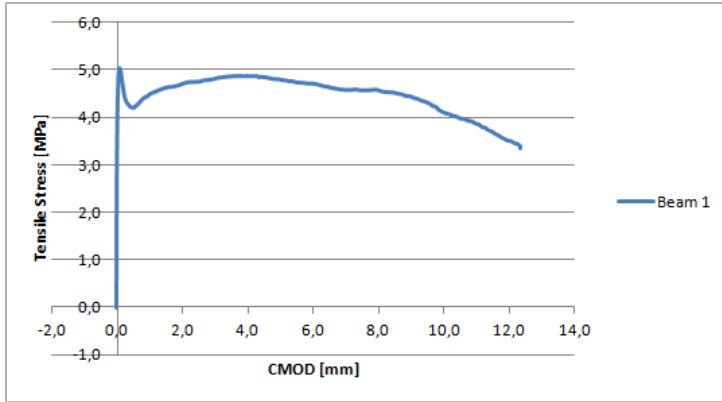
Figure 5.6: *Tensile stress - CMOD relationship for standard beam*
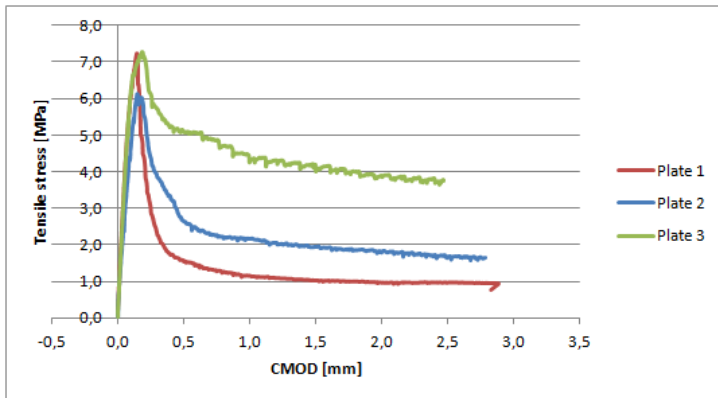
Figure 5.7: *Tensile stress - CMOD relationship for plates*

Specimen	F_L [kN]	$f_{ct,L}^f$ [N/mm^2]	$f_{R,1}$ [N/mm^2]	$f_{R,2}$ [N/mm^2]	$f_{R,3}$ [N/mm^2]	$f_{ftk,res,2,5}$ [N/mm^2]
Beam 1	14.65	5.04	4.21	4.62	4.75	1.758
Plate 1	4.61	7.26	1.57	1.04	0.98	0.362
Plate 2	4.13	6.04	2.64	1.95	1.67	0.618
Plate 3	4.33	7.26	5.08	4.03	3.74	1.385
Average	**4.36**	**6.85**	**3.10**	**2.34**	**2.13**	**0.789**

Table 5.2: *Results from beam testing*

5.4 Discussion

5.4.1 Cylinder Test

The average compressive strength of the concrete cylinders is 41 N/mm^2. This is higher than the value 30 N/mm^2 which is from Eurocode 2 and used in design calculations. However, this value is conservative. In addition the fibre reinforced concrete is known to have a higher compressive strength than regular concrete, as the fibres help increase the compressive strength. There is no pronounced difference between the highest and lowest value obtained from the test.

5.4.2 Beam test

The residual tensile strength $f_{ftk,res,2,5}$ for the standard beam is 1.58 N/mm^2, while the average for the plates is 0.79 N/mm^2. However, there are great differences between the three plates. Plate 1 and 2 have quite low residual tensile strengths (0.36 and 0.62 N/mm^2) while plate 3 has a residual tensile strength of 1.39 N/mm^2. Ideally the residual tensile strength should be the same independent of thickness.

The variation in this case can be caused by different reasons. While the standard beam is tested according to NS-EN 14561, the plates are tested according to the Norwegian Sawn Beam Test (NSBT). Because of the notch sawn in NS-EN 14561 the beam is bound to crack in this section. As there is no notch in the NSBT, the cracking will occur in the weakest section. This often gives a higher residual tensile strength when using the NS-EN 14561 test compared to the NSBT. It can also explain the large deviations between the plates, as the weakest section varies depending on orientation and spreading of the fibres.

Another reason for the variance is that the higher the testing beam is, the more likely is it that the fibres sink to the bottom rather than spread throughout the section. This gives a higher fibre content in the tensile zone, and thus a higher tensile strength.

Preferably there should have been several standard beams for testing to give a more comprehensive result. Unfortunately due to lack of concrete during casting there was only one made. This gives a poor basis for comparison with the plates, and it is difficult to know if the tensile strength from the beam is a representative value. Nordbrøden and Weydahl (2012) looked at shear capacity in fibre reinforced concrete beams. They obtained a residual tensile strength of 4.0 N/mm^2 with a fibre content of 80 kg/mm^3. It can be assumed that the residual tensile strength increases proportionally with the amount of fibre by small amounts. As Nordbrøden and Weydahl describes their value as higher than expected, the value obtained in this thesis thus is seen as reasonable.

6 | Results

This chapter presents the results from the shear test, the dynamic impact test and the deflection test

6.1 Shear test

The test was carried out May 23rd 2013 at NTNU. Figure 6.1 shows the shear force-slip relationship of the two specimens tested. Specimen 1 was unloaded at a higher load than specimen 2 because the estimated maximum load was first assumed to be 80 kN. This was adjusted when testing specimen 2. The slip modulus k is in this case the slip modulus for the SLS (the same as k_{ser} defined by Ceccotti). As all testing was done within SLS no slip modulus was determined for the ULS. The results from the shear test indicates a ductile behaviour for the shear connector. Figure 6.1 shows a stiff connection until approximately 20 kN where the connection starts to yield and with a more gradual slope reaches the ultimate load of 53 kN. The deformations are quite big, with a 9 mm slip at ultimate load.

The shear force-slip plots are used to find the stiffness of the shear connector, based on the elastic regions of the curves. This stiffness is further used in the thesis to explain the behaviour of the timber-concrete composite beam. Table 6.1 presents the stiffness, ultimate load and the slip at ultimate load for the 2 specimens.

Specimen	Slip modulus k [kN/mm]	Ultimate load F_{max} [kN]	Max slip u [mm]
1	191.88	52.85	9.67
2	239.87	52.83	8.98
Average	*215.87*	*52.84*	*9.33*

Table 6.1: *Results from shear test; slip moduli and shear strength*
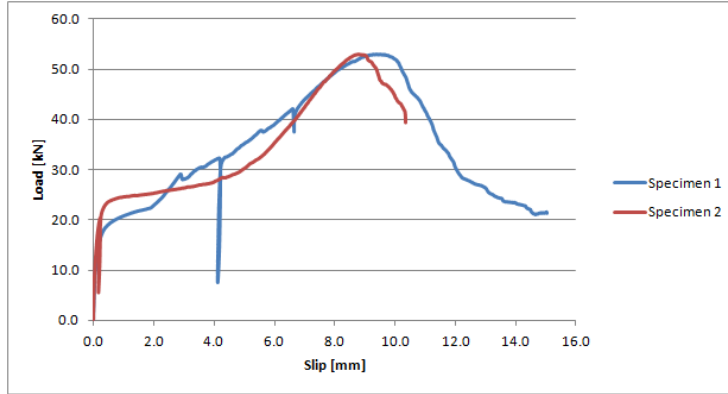
Figure 6.1: *Results from shear test*

6.2 Dynamic impact test

Tests were carried out at NTNU May 6th 2013. The first five mode shapes and frequencies are taken into consideration. Table 6.2 shows the mode shapes found in LabVIEW and a description of the modes.

Table 6.3 shows the natural frequencies f and damping ratios found from the impact test. Test 1,2 and 3 refers in this case to the three different placements of the accelerometer during the impact testing. Test 1 is with the accelerometer placed underneath Beam N, test 2 is with the accelerometer placed underneath Beam S, while test 3 is with the accelerometer placed in the concrete span. For mode 3 there are two frequencies listed in the table. This is due to LabVIEW finding two frequencies with a similar mode shape. For test 3 only mode 1, 3 and 5 were recorded, meaning there are no vibrations within the concrete deck.

The test showed an average frequency of 11.98 Hz in the first mode and an average damping of 0.858%. It was experienced some difficulties of estimating the damping ratios through LabVIEW, with different damping ratios depending on the approach.
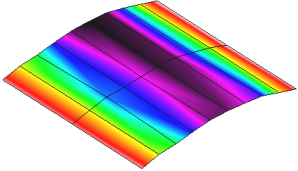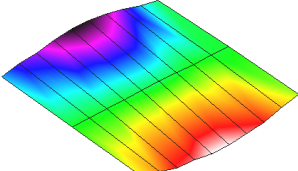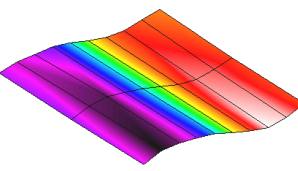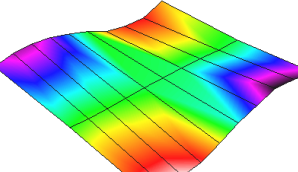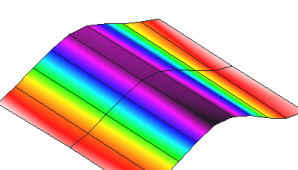
Mode number	LabVIEW	Description
Mode 1		1st bending mode, symmetrical bending
Mode 2		1st bending mode, asymmetrical bending
Mode 3		2nd bending mode, symmetrical bending
Mode 4		2nd bending mode, asymmetrical bending
Mode 5		3rd symmetrical bending

Table 6.2: *Identified mode shapes*

Mode number	Test 1		Test 2		Test 3	
	f [Hz]	Damping [%]	f [Hz]	Damping [%]	f [Hz]	Damping [%]
Mode 1	12.413	0.831	12.127	0.854	11.397	0.970
Mode 2	15.683	0.898	15.364	0.883	-	
	29.242	0.849	29.027	1.028		
Mode 3	34.670	0.507	34.976	0.687	33.435	0.578
Mode 4	41.886	0.989	41.043	0.950	-	
Mode 5	50.951	0.591	50.735	0.742	50.855	0.895

Table 6.3: *Frequencies and damping ratios of the five first modes*

	Deflection [mm]		
Load case	Beam N	Beam S	Concrete span
1	0.2359	0.2433	-
2	0.3309	0.147	-
3	0.2455	0.2541	0.021

Table 6.4: *Deflection at 1 kN load*

6.3 Deflection test

The test was carried out at NTNU May 15th 2013. Table 6.4 shows the deflection of the beam at the three load cases from section 4.5. The deflection of the concrete span in load case 3 is the net deflection. The test showed a deflection of about 0.24 mm under a 1 kN load, with beam S having some larger deflections than beam N. The deflection of the concrete span was 0.021 mm.

7 | Evaluation and comparison of experimental and numerical results

In this chapter, the results from the dynamic impact test, the deflection test and the shear test are evaluated and compared with the results from the analysis done ABAQUS.

7.1 Shear strength and slip modulus

The type of shear connector used in this thesis was chosen based on previous research done on similar connections. Both Lukaszewska (2009), Bathon and Bletz (2006) and Clouston et al. (2005) all got a high slip moduli, high ultimate load and small relative slip using a glued-in continuous steel mesh as shear connector. Compared to them, the connector used in this thesis shows a quite different behaviour. Table 7.1 presents the results from this thesis together with those of Lukaszewska (2009), Bathon and Bletz (2006) and Clouston et al. (2005).

Research	Slip modulus k [kN/mm]	Ultimate load F_{max} [kN]	Max slip u [mm]
Shear test	215.87	52.84	9.33
Lukaszewska (2009)	483.8	81.2	4.0
Clouston et al. (2005)	415.46	111.62	1.44
Bathon and Bletz (2006)	415	90	1.4

Table 7.1: *Comparison of shear test results. Bathon and Bletz's results are only approximate*

Figure 7.1: *The failure mode of the shear connector*

Lukaszewska, Bathon and Graf, and Clouston et al. all characterized the failure mode as brittle. As seen in table 7.1 the slip moduli is approximately double of the slip moduli obtained from this thesis. The same applies for the ultimate load. The deformations are also much smaller for the comparing tests. Fig 7.1 shows the failure of the test specimen. The steel mesh has yielded and then teared at the line of the concrete. An important thing to notice is that the slot is not entirely filled with epoxy glue. The gap between the glue and the concrete is at places up to 15 mm, leaving a big part of the steel mesh exposed. This is assumed to be the reason for the ductile behaviour. After a certain point during loading, the steel mesh will collapse sideways and is then only subjected to tensile forces. The steel strands will tear when the tensile forces get too high. This coincides well with the shear force-slip relationship shown in figure 6.1.

Precision while gluing is therefore essential for obtaining a high stiffness of the tested shear connector. However, also other issues could improve its behavior. The mesh was oriented so that the long way of the mesh was turned vertically. Estimates showed the mesh would have about three times as high capacity if the long way of the mesh was turned horizontally. In the case of a small gap this would not be significant. Only a small part of the mesh would be exposed, and the forces would come as shear in the steel strands. With a gap as big as the one discovered in the shear test, the forces will create bending in the mesh at top and bottom which leads to the collapse. In this case the horizontally oriented mesh resists much bigger forces. Also, the concrete elements were cast so the rough surfaces were facing down towards the glulam joists. Irregularities on the surface caused for some elements a bigger gap between the concrete and

46

the glulam. At last it can be discussed if the steel mesh and the fibre reinforced concrete is a good combination. The events of cracking during the construction of the composite beam could be due to the fibres not being able to penetrate the mesh.

The FE model was used to estimate the stiffness of the shear material used as the connector in the full-scale model. By decreasing the modulus of elasticity in the shear material to 10000 N/mm^2 it was possible to obtain the same stiffness as found through the shear tests. This value was used for the other numerical models. Numerical analysis showed the failure was most likely to occur in the steel mesh close to the concrete which proved to correct. However, the FE model for the shear test is not good for estimating behaviour, as the shear material is modelled as a plate instead of a grid.

7.2 Dynamic behaviour

According to Eurocode 5 a floor with a natural frequency less than 8 Hz requires special investigation. Through the tests described in section 4.4 the average natural frequency of the first mode is 11.98 Hz. The composite beam is thus regarded as above the critical area for uncomfortable vibrations. The vibration criteria stated by Hu and Chui (2004) and found in eq. 4.1 is also fulfilled. This is shown by inserting the natural frequency and the average deflection for load case 1 from table 6.4. The dimensioning value when designing the beam was 13.94 Hz, i.e. a little over what was found from the hammer impact test.

There is a discussion whether damping found through simple tests have any relevancy to a full-size floor. Several studies have concluded that furnishing and non-structural components influence the damping ratio more than the construction itself (Lukaszewska, 2009). There is also a general lack of trust in measurement methods (Labonnote et al., 2012). Also in this thesis the estimation of damping ratios was found difficult.

Labonnote et al. (2012) did a series of experiments to determine the frequency and damping ratio of timber beams with different spans and orientation. The glulam beams used in the research had a cross-section of 88 x 404 mm^2, approximately equal to the glulam joists in this thesis. A tendency found was that for the higher modes and shorter spans the damping ratio was larger. This, however, was more apparent for facewise oriented beams. Also, Labonnote et al. (2012) states that the dependence of the damping ratio on the mode number decreases with an increasing span. E.g., the damping ratios presented in this

thesis did not show such dependency. Looking at the modes with symmetrical bending only (mode 1, 3 and 5), there is a decrease in the average damping ratio from 0.86% to 0.64% between mode 1 and 3. Between mode 3 and 5 the average damping ratio increases to 0.73%.

As a comparison Lukaszewska (2009) tested two full-scale timber-concrete composite beams with different shear connectors for dynamic properties. The beams were 4.8 m. The natural frequencies for the first mode were 18.5 and 18.9 Hz, while they for the second mode were 24.8 and 25.0 Hz. The damping ratios were 7.3% and 7.1% for mode 1 and 6.7% and 7.5% for mode 2. Lukaszewska does not describe the mode shapes so it is difficult to compare the values, but it is reasonable to assume that at least the first mode is the same for both tests.

Deam et al. (2008) tested five different timber-concrete composite beams for frequency and damping. The span of the beams were 6 m. The frequency varied from 17.1-19.3 Hz, while the damping varied from 1.3-2.3%. Only the first mode was evaluated.

Comparing these results can only be done indicatively as the natural frequency is a function of mass, stiffness and length of the span. Equation 4.2 shows that with a higher mass and longer span the frequency will decrease. This coincides well if these results are compared with the frequencies of the composite beam tested in this thesis. With a longer span, the frequency is lower than those found by Lukaszewska and Deam et al. It may be questioned whether the damping ratios from Lukaszewska are reasonable, as they are quite high compared to the damping ratios obtained both in this thesis and by Deam et al. Compared to the damping ratios found by Deam et al. (2008) the values found through testing seem reasonable. They are a little lower, but according to Labonnote et al. (2012) the damping ratio will increase with shorter spans.

To verify the results from the hammer impact test a dynamic analysis was done in ABAQUS. Table 7.2 shows the mode shapes found through the numerical analysis and identified as the same mode shapes as in table 6.2. In figure 7.2b the frequencies from the experimental part are compared with those found from ABAQUS. "Numerical" are the values found from using the same stiffness as determined through the experimental tests. "Numerical FCA" are the frequencies found when using an "infinite" stiffness, i.e. full composite action. The frequencies from ABAQUS coincide well with those from the impact test. For the first mode there is a discrepancy of 2.2% between the empirically determined and modelled frequency, where ABAQUS estimates the frequency to 11.72 Hz. The numerical model with full composite action shows an increase in frequency
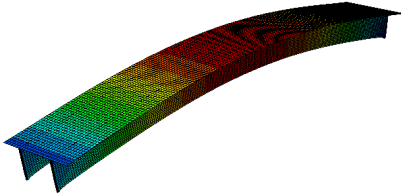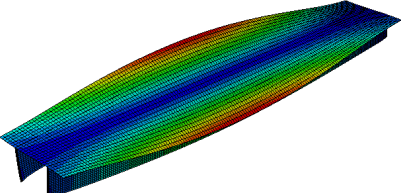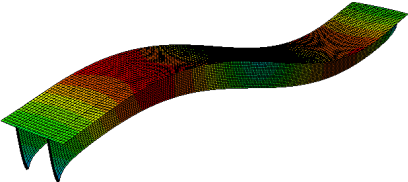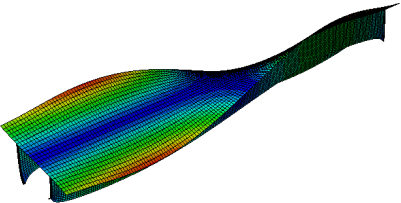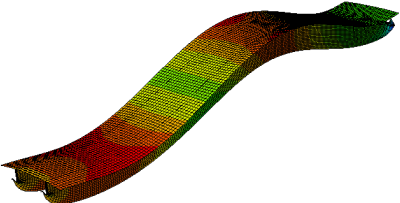
Mode number	ABAQUS	Description
Mode 1		1st bending mode, symmetrical bending
Mode 2		1st bending mode, asymmetrical bending
Mode 3		2nd bending mode, symmetrical bending
Mode 4		2nd bending mode, asymmetrical bending
Mode 5		3rd symmetrical bending

Table 7.2: *Mode shapes from ABAQUS*
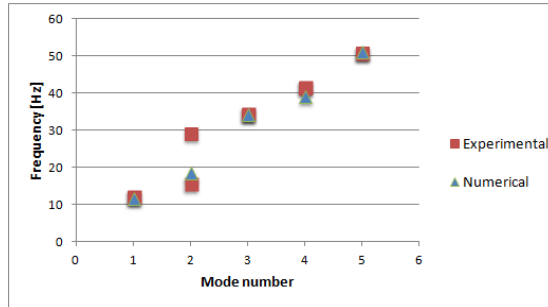
(a)
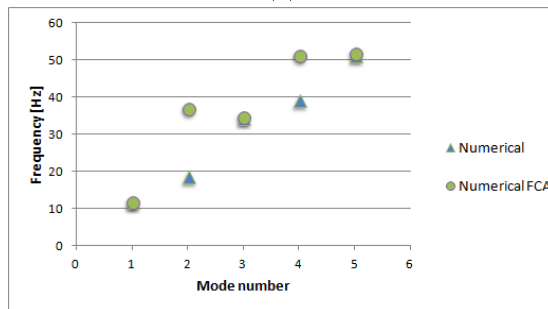
(b)

Figure 7.2: *Comparison of the empirically determined and modelled frequencies (a), and comparison of the modelled frequencies for FCA and PCA (b)*

mainly in the modes with asymetrical bending. It was discussed if this could be due to the torsional stiffness in the connection being more affected by the increase in stiffness than the bending stiffness.

For the second mode there were two frequencies from the testing that could be identified as belonging to that mode. Both differs from the numerical frequency of 18.65 Hz. It was not discovered what caused this. Doing an analysis with different slip moduli in the two glulam joists showed an increase in the frequency in the second mode, but does not explain the two similar mode shapes.
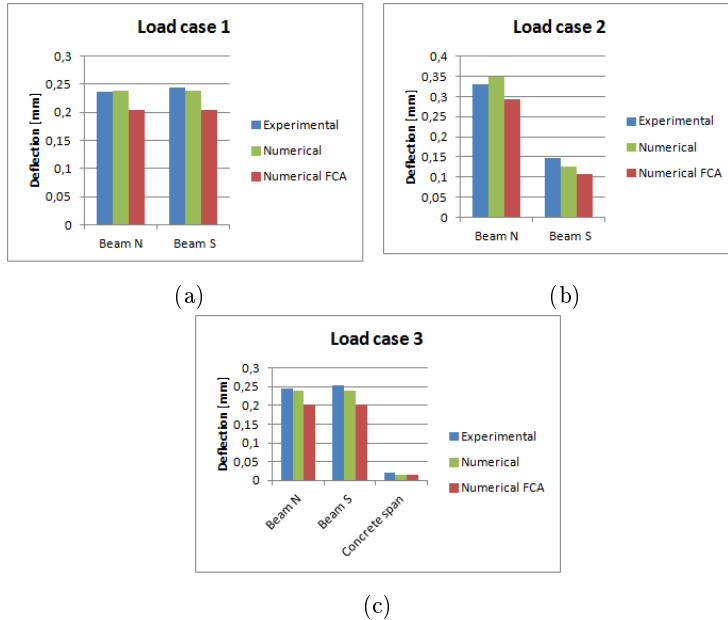
Figure 7.3: *Deflections during load case 1 (a), load case 2 (b) and load case 3 (c). "Numerical" refers to the analysis done with a stiffness equal to the one found from the shear test, while "Numerical FCA" refers to the analysis done with an infinite stiffness.*

7.3 Deflection and bending stiffness

The deflections found in section 6.3 are helpful to find the effective bending stiffness and the grade of composite action of the composite beam. In figure 7.3 the deflections from the test are compared to those found through numerical analysis in ABAQUS. As seen the empirically determined deflections are similar to those from ABAQUS. For the numerical analysis done with full composite action the deflections are about 16% lower.

The biggest discrepancy between the empirically determined and the numerical values is found in load case 2. ABAQUS estimates a larger deflection for the glulam joist where the load is applied (Beam N) and a smaller deflection on the opposite joist (Beam S). The concrete material in ABAQUS does not contain

any form of reinforcement, therefore the fibre reinforced concrete is most likely transferring the deflections better than what the concrete does in the numerical analysis.

Also for the deflection in the concrete span there are some discrepancy. In the deflection test it was recorded a net deflection of 0.021 mm while it from the numerical analysis was found a net deflection of 0.016 mm. This is probably due to the fact that the FE model is not modelled with en epoxy layer between the concrete elements, but a rigid connection. If comparing to the theoretical deflection of a single simply supported concrete element, the deflection is 0.026 mm. This means the deflection from the test places itself in between, which is reasonable.

However, it has to be emphasized that the deflections found in this test are very small, and that the differences found may as well be caused from inaccuracies in measuring devices or the FE model.

From the deflections in load case 1 it was possible to calculate the effective bending stiffness and composite action of the timber-concrete composite beam. Using equation 3.1 it was found a composite action of 61%. This was compared to the theoretical composite action using the stiffness derived from the shear test and Eurocode 5 Annex B, which gave 68% composite action. Both values are lower than anticipated, primarily due to the low slip modulus of the shear connector. It must be still be pointed out that a composite action of over 60% is not bad, and several other type of connectors are less strong (Lukaszewska, 2009).

7.4 Expansion to a full-size floor

A FE model of a full-size floor (8x6 m) was analyzed to see if there was any pronounced differences in frequencies between the two models. One analysis was done with the same stiffness as the one found through the shear test, and one with full composite action. Only the first mode was examined. Figure 7.4 shows the mode shape of the floor. ABAQUS estimated the frequency to 12.92 Hz for the floor with the original stiffness, and 14.86 Hz for the floor with full composite action. In both cases this was an increase in frequency, from 11.72 Hz and 11.99 Hz, respectively. This coincides with the statement from Deam et al. (2008) that the frequency will increase when several units are coupled together.

52
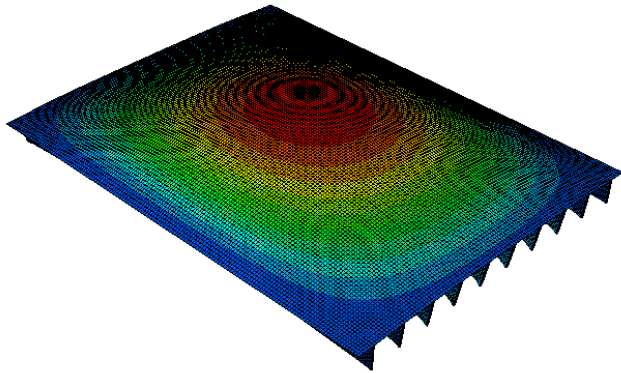
Figure 7.4: *First mode of the full-size floor FE model*

8 | Conclusions and future research

This chapter presents the conclusions drawn form the work of this thesis, as well as suggestions for further work

8.1 Conclusions

The aim for this thesis was to look at timber-concrete composite structures in floors. A system with concrete elements instead of a continuous concrete slab was developed. The steel mesh chosen as a shear connector was similar to some used in previous studies, which had proved to be stiff and achieve almost full composite action. By looking at the dynamic performance of a timber-concrete composite beam the goal was to say something about the area of application of this type of structures.

The shear connector proved to be stiff, though not as stiff as the similar connections. The connector showed large deformations before reaching the ultimate load. This was mostly due to insufficient gluing, but could partly have been avoided by turning the direction of the steel mesh. It can also be questioned if a steel mesh shear connector and fibre reinforced concrete was a good combination. During the work with the concrete elements it was discovered that the fibres did not spread well through the steel mesh. If deciding to use the steel mesh in fibre reinforced concrete special attention and care should be paid to this area.

Both the fibre reinforced concrete and the epoxy glue performed satisfying according to their expectations. The concrete elements tested had a very varying residual tensile strength, but the average value was within the capacity of the ULS design load. The epoxy glue proved very strong in the shear tests. However the gluing between the concrete elements were not tested in any specific way.

The hammer impact test determined the frequency of the first mode as 11.98 Hz, above the critical area for floor vibrations. Numerical analysis with ABAQUS gave accurate estimates. It was also shown that increasing the composite action would not increase the frequency of the first mode in any pronounced way.

Looking at the deflections for 1 kN load the effective bending stiffness and the efficiency of the composite beam was computed. Comparing with the numerical analysis, the experimental values gave very similar results. The ABAQUS solution for full composite action showed that the deflections could be decreased with around 16%. The ABAQUS model was deemed adequate for estimating the performance of the timber-concrete composite beam. Expanding the ABAQUS model to a full floor gave higher values for the frequency in the first mode.

In general the timber-concrete composite beam showed a satisfactory behaviour in terms of vibration and stiffness. Some modifications should be done on the shear connector, and further research is needed. The concept used in this thesis proved to be quite applicable. The assembling of the composite beam went smoothly, and the concrete elements were relatively manageable to move. Precision is needed in the creation of the concrete elements though, as the shear connectors have to be placed equally in every element. Also, the use of epoxy glue requires a fast and unproblematic assembly, and the costs are quite high. There has to be en evaluation whether increased composite action is worth the extra costs and effort if this specific floor is to be developed.

8.2   Future research

This thesis has only touched down on some subjects concerning timber-concrete composite floors. To fully understand the behaviour of a timber-concrete composite floor, several subjects have to be investigated.

All tests done on the full-scale beam, as well as numerical analyses and analytical calculations, assumed a simply supported beam. In a floor construction this is not realistic, and it should be investigated how the rotational stiffness at the supports affects frequency and damping.

Another important issues not followed up in this thesis is the long-term effects of the floor. Timber is especially prone to creep as an effect of long-term loading and relative humidity, and it is relevant to look at the time-dependent behaviour of composite beams when it comes to deflections.

As mentioned above, the performance of the concrete elements was not examined further. If the concept of concrete elements should be elaborated this must be done, i.e. with a comparison to the alternative with a continous concrete slab. It is also necessary to find a way to connect the concrete elements to each other in the transverse direction.

Bibliography

L. Bathon and O. Bletz. Long term performance of continous wood-concrete-composite systems. In 9th *World Conference on Timber Engineering WCTE 2006, Portland, Oregon, USA*, 2006.

L. Bathon and M. Graf. A continous wood-concrete-composite system. In 6th *World Conference on Timber Engineering WCTE 2000, Whistler Resort, British Columbia, Canada*, 2000.

L. Bathon, O. Bletz, and J. Schmidt. Hurricane proof buildings - An innovative solution using prefabricated modular wood-concrete-composite elements. In 9th *World Conference on Timber Engineering WCTE 2006, Portland, Oregon, USA*, 2006.

A. Ceccotti. Composite structures. In H. J. Blass, P. Aune, B. S. Choo, R. Görlacher, D. R. Griffiths, and B. H. Hilson, editors, *Timber Engineering-STEP 2*, chapter E13. Centrum Hout, The Netherlands, 1995.

A. Ceccotti, M. Fragiacomo, and S. Giordano. Long-term and collapse tests on a timber-concrete composite beam with glued-in collection. *Materials and Structures*, 2007.

P. Clouston, L. Bathon, and A. Schreyer. Shear and bending performance of a novel wood-concrete composite system. *ASCE Journal of Structural Engineering*, 2005.

R. Crocetti, T. Sartori, and Flansbjer M. Timber-concrete composite structures with prefabricated frc slab. In 11th *World Conference on Timber Engineering WCTE 2010, Riva del Garda, Italy*, 2010.

I. M. Daniel and O. Ishai. *Engineering mechanics of composite materials*. Oxford University Press, 2006.

B. L. Deam, M. Fragiacomo, and L. S. Gross. Experimental behaviour of prestressed lvl-concrete composite beams. *Journal of Structural Engineering*, 2008.

L. J. Hu and Y. H. Chui. Development of a design method to control vibrations induced by normal walking action in wood-based floors. In 8th *World Conference on Timber Engineering WCTE 2004, Lahti, Finland*, 2004.

T. Kanstad. *Forslag til retningslinjer for dimensjonering, utførelse og kontroll av fiberarmerte betongkonstruksjoner.* Concrete Innovation Centre (COIN), 2011.

H. Kreuzinger. Mechanically jointed beams and columns. In H. J. Blass, P. Aune, B. S. Choo, R. Görlacher, D. R. Griffiths, and B. H. Hilson, editors, *Timber Engineering-STEP 1*, chapter B11. Centrum Hout, The Netherlands, 1994.

N. Labonnote, A. Rønnquist, and K. A. Malo. Experimental study on material damping in timber beams. In 12th *World Conference on Timber Engineering WCTE 2004, Lahti, Finland*, 2012.

E. Lukaszewska. *Development of Prefabricated Timber-Concrete Composite Floors.* PhD thesis, University of Luleå, Sweden, 2009.

Mapei. Mapepoxy l-ls-lr. `http://www.mapei.com/NO-NO/products-subline.asp?IDLinea=108`, February 2012.

C. B. McCullough. Oregon tests on composite (timber-concrete) beams. *Journal of the American Concrete Institute*, 1943.

Moelven. Karakteristiske fastheter, limtre og smalt limtre. `http://www.moelven.com/Documents/Limtre/Fastheter`, November 2012.

H. H. Nordbrøden and S. H. Weydahl. Testing of fibre reinforced concrete structures. shear capacity of beams with corbel-end. Master's thesis, NTNU, 2012.

F. E. Richart and C. B Williams. Tests of composite timber-concrete beams. *Journal of the American Concrete Institute*, 1943.

S. Sandbakk. *Fibre Reinforced Concrete. Evaluation of test methods and material development.* PhD thesis, NTNU, Norway, 2011.

Standard Norge. *EN 26891:1991. Timber structures. Joints with mechanical fasteners. General principles for the determination of strength and deformation characteristics.* European Committee for Standardization, 1991.

Standard Norge. *NS-EN 12390:2012. Test method for metallic fibre concrete. Measuring of the flexural tensile strength (limit of proportionality (LOP), residual).* European Committee for Standardization, 2005.

Standard Norge. *Eurocode 1 - Actions on structures. Part 1-1: General Actions. Densities, self-weight, imposed loads for buildings. NS-EN 1991-1-1:2002+NA:2008.* European Committee for Standardization, 2008a.

Standard Norge. *Eurocode 2 - design of concrete structures - part 1-1: General rules and rules for buildings. NS-EN 1992-1-1:2004+NA:2008.* European Committee for Standardization, 2008b.

Standard Norge. *Eurocode 5 - design of timber structures - part 1-1: General rules and rules for buildings. NS-EN 1995-1-1:2004+A1:2008+NA:2010.* European Committee for Standardization, 2010.

Standard Norge. *NS-EN 14651:2005. Testing hardening concrete.* European Committee for Standardization, 2012.

APPENDIX

Appendix A

Calculations of composite beam, EC5 Annex B
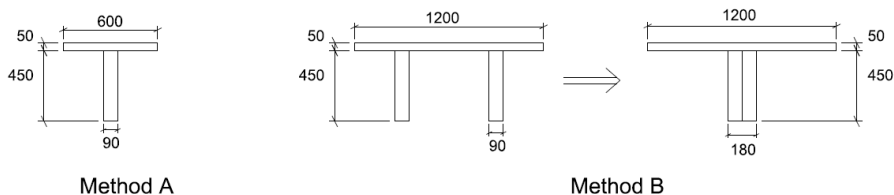
Method A

Method B

Example Method A

Concrete

Width	$b_1 = 600$ mm
Height	$h_1 = 50$ mm
Area	$A_1 = 30000$ mm^2
Moment of inertia	$I_1 = 6.25e6$ mm^4
Modulus of elasticity	$E_1 = 30000$ N/mm^2
Density	$\rho_1 = 2400$ kg/m^3

Glulam

Width	$b_2 = 90$ mm
Height	$h_2 = 450$ mm
Area	$A_2 = 40500$ mm^2
Moment of inertia	$I_1 = 6.83e8$ mm^4
Modulus of elasticity	$E_2 = 13000$ N/mm^2
Density	$\rho_2 = 470$ kg/m^3

Load

Self weight per m	$G = 9.81 * (A_1\rho_1 + A_2\rho_2)/1000^3$ kN/m $= 0.865$ kN/m
Design load	$q = 2.4$ kN/m
Total load SLS	$Q_{SLS} = 3.27$ kN/m
Design moment	$M = 26.1$ kNm
Design shear force	$V = 26.1$ kN

Shear stiffness ULS	$k = 415$ kN/mm
Spacing	$s = 500mm$
Shear coefficients	$\gamma_1 = [1 + \pi^2 E_1 A_1/(kl^2))]^{-1} = 0.845$
,	$\gamma_2 = 1.0$

a	$a = h_1/2 + h_2/2 = 250$ mm
a_2	$a_2 = \gamma_1 E_1 A_1 (h_1 + h_2)/[2(\gamma_1 E_1 A_1 + \gamma_2 E_2 A_2)] = 153.4$ mm
a_1	$a_1 = a - a_2 = 96.6$ mm

Efficient bending stiffness	$(EI)_{ef} = E_1 I_1 + \gamma_1 E_1 A_1 a_1^2 + E_2 I_2 + \gamma_2 E_2 A_2 a_2^2$
,	$= 2.93e13$ N/mm^2

Stresses

Normal stresses concrete	$\sigma_1 = \gamma_1 E_1 a_1 M/(EI)_{ef} = 3.4$ MPa
,	$\sigma_{m,1} = 0.5 E_1 h_1 M/(EI)_{ef} = 1.0$ MPa
Compression strength concrete	$\sigma_{c,1} = \sigma_1 + \sigma_{m,1} = 4.5$ MPa $< f_{cd}$ OK
Tensile strength concrete	$\sigma_{t,1} = \sigma_{m,1} - \sigma_1 = -2.4$ MPa $< f_{ctd,0,05}$ OK

Normal stresses glulam	$\sigma_2 = \gamma_2 E_2 a_1 M/(EI)_{ef} = 2.5$ MPa
,	$\sigma_{m,2} = 0.5 E_2 h_2 M/(EI)_{ef} = 3.7$ MPa
Combined bending and tension criteria	$\sigma_2/(k_h f_{t0d}) + \sigma_{m,2}/(k_h f_{md})$
,	$= 0.37 < 1.0$ OK

Maximum shear stress	$\tau_{2,max} = 0.5 E_2 h_2^2 V/(EI)_{ef} = 0.83$ MPa $< f_{vd}$ OK

CE L40C

			med. Load		
Bøyning	fmk	N/mm2	21.4	fmd	30.8
Strekk	ft0k	N/mm2	12.2	ft0d	17.6
	ft90k	N/mm2	0.3	ft90d	0.4
Trykk	fc0k	N/mm2	17.7	fc0d	25.4
	fc90k	N/mm2	1.9	fc90d	2.7
Skjær	fvk	N/mm2	2.4	fvd	3.5
E-modul	E0mean	N/mm2	9043	E0d	13000
	E0,05	N/mm2	7304	E0,05d	10500
	E90mean	N/mm2	285	E90d	410
Skjærmodul	G0mean	N/mm2	529	G0d	760
Densitet	ρk	kg/m3	400		
	ρmean	kg/m3	470		

B30-R3

Trykkfasthet	fck	N/mm2	30	fcd	17
	fckcube	N/mm2	37	fcdcube	21
Strekkfasthet	fctk0,05	N/mm2	2	fctd0,05	1.3
Rest strekkfasthet	fftk,res2,5	N/mm2	3	fftd,res2,5	2
Rest bøyestrekkfasthet	fR,3	N/mm2	8.1	fR,3	
E-modul	Ecm	N/mm2	33000	Ecm	
Densitet	ρk	kg/m3	2400		

	CE L40C	B30-R3
Partial factor	1.15	1.5
kmod,perm	0.6	0.6
kmod,mellom	0.8	0.8
kdef	0.6	0.6

Concrete / Giulam

	t [mm]	A [mm2]	I [mm4]	g1 [kN/m]	h [mm]	b [mm]
	50	30000	6250000	0.706	450	450
	50	60000	12500000	1.413	450	450

Load

I [mm4]	g2 [kN/m]	q [kN/m]	6.10a	6.10b	Quls [kN/m]	Qsls [kN/m]	M [kNm]	V [kN]
40500	0.159	2.4	3.69	4.64	4.64	3.27	37.1	18.6
81000	0.318	2.4	4.86	5.68	5.68	4.13	45.4	22.7

Connector / Compaction

Method	kser [kN/mm]	ku [kN/mm]	A [mm2]	I [mm4]	γ1	a
A)	480	415	600	6250000	0.8446	250
A)	216	180	180		0.7022	250
B)	216	180	180		0.5411	250
A - FCA)	-	-			1.0000	250
B - FCA)	-	-			1.0000	250

Method	EI_eff [Nmm2]	a1	a2	σ1	σm1	σ2	σm2	σt2max	σc1	σt1	M [kNm]	V [kN]
A)	2.928E+13	96.6	153.4	3.4	1.0	2.5	3.7	0.834	4.5	-2.4	1.03	0.37
A)	2.782E+13	107.7	142.3	3.3	1.1	2.5	3.9	0.878	4.4	-2.2	1.03	0.37
B)	5.137E+13	123.9	126.1	2.0	0.7	1.4	2.6	0.582	2.7	-1.2	1.03	0.23
A - FCA)	3.057E+13	86.8	163.2	3.5	1.0	2.6	3.6	0.799	4.5	-2.5	1.03	0.37
B - FCA)	6.115E+13	86.8	163.2	2.1	0.6	1.6	2.2	0.489	2.7	-1.5	1.03	0.22

Vibration — NB! Enhetslast!!!

	w [mm]	f [1/s]	criteria >1
A)	0.187	13.95	2.746
A)	0.201	13.45	2.349
B)	0.224	12.74	1.864
A - FCA)	0.174	14.45	3.193
B - FCA)	0.174	14.45	3.193

F [kN]	γ1_SLS	EI_eff SLS
25.6	0.7587	2.849E+13
25.0	0.5859	2.648E+13
29.3	0.4143	4.752E+13
26.1	1.0000	3.057E+13
31.9	1.0000	6.115E+13

Effiency

r1	r2	E0	EI0	EI∞	η
83.3	83.3	166.7	9.091E+12	3.059E+13	0.902
83.3	83.3	166.7	9.091E+12	3.059E+13	0.809
83.3	83.3	166.7	1.818E+13	6.118E+13	0.682
83.3	83.3	166.7	9.091E+12	3.059E+13	0.999
83.3	83.3	166.7	1.818E+13	6.118E+13	0.999

Appendix B

Translation to stiffness parameters for a transversely isotropic material

The following procedure is taken from Daniel and Ishai (2006), and show the derivation of the stiffness parameters used in ABAQUS. The material parameters used for glulam CE l40C:

E_x	E_y	ν_{xz}	ν_{xz}	ν_{xy}	G_{zy}
13000	410	0.6	0.6	0.6	760

The stiffness parameters are related to stress and strains through the following relationship:

$$[\sigma] = [C][\epsilon]$$

where [C] is the matrix containing the stiffness parameters. For a transversely isotropic material the matrix looks like this:

$$M = \begin{bmatrix} C_{11} & C_{12} & C_{12} & 0 & 0 & 0 \\ C_{12} & C_{22} & C_{23} & 0 & 0 & 0 \\ C_{12} & C_{23} & C_{22} & 0 & 0 & 0 \\ 0 & 0 & 0 & (C_{22} - C_{23})/2 & 0 & 0 \\ 0 & 0 & 0 & 0 & C_{55} & 0 \\ 0 & 0 & 0 & 0 & 0 & C_{55} \end{bmatrix}$$

where the stiffnesses are related to the engineering constants in the following way:

$$C_{11} = \frac{1 - \nu_{23}\nu_{32}}{E_2 E_3 \Delta}$$

$$C_{22} = \frac{1 - \nu_{13}\nu_{31}}{E_1 E_3 \Delta}$$

$$C_{12} = \frac{\nu_{21} + \nu_{31}\nu_{23}}{E_2 E_3 \Delta} = \frac{\nu_{12} + \nu_{13}\nu_{32}}{E_1 E_3 \Delta}$$

$$C_{23} = \frac{\nu_{32} + \nu_{12}\nu_{31}}{E_2 E_3 \Delta} = \frac{\nu_{23} + \nu_{21}\nu_{13}}{E_1 E_2 \Delta}$$

$$C_{55} = G_{xy}$$

The answers are obtained from the following MATLAB script:

```
Ex=13000;
Ey=410;
Ez=Ey;

vxz=0.6;
vxy=0.6;
vzy=0.6;
Gxz=760;
Gxy=Gxz;


vyx=Ey*vxy/Ex
vzx=Ez*vxz/Ex
vyz=Ey*vzy/Ez

Delta=[1 -vzx -vyx; -vxz 1 -vyz; -vxy -vzy 1];

d=1/(Ex*Ez*Ey)*det(Delta);

C11=(1-vzy*vyz)/(Ez*Ey*d);
C22=(1-vxy*vyx)/(Ex*Ey*d);
C12=(vxz+vxy*vyz)/(Ex*Ey*d);
C13 = C12;
```

```
C33 = C22;
C23=(vzy+vzx*vxy)/(Ex*Ez*d);
C44=(C22-C23)/2;
C55=Gxy;
C66 = C55;


C=[C11 C12 C13 0 0 0;
C12 C22 C23 0 0 0;
C13 C23 C33 0 0 0;
0 0 0 C44 0 0;
0 0 0 0 C66 0;
0 0 0 0 0 C55]


C =

   1.0e+04 *

   1.3782    0.0652    0.0652         0         0         0
   0.0652    0.0671    0.0415         0         0         0
   0.0652    0.0415    0.0671         0         0         0
        0         0         0    0.0128         0         0
        0         0         0         0    0.0760         0
        0         0         0         0         0    0.0760
```

The values used in ABAQUS:

D1111	13782
D1122	652
D2222	671
D1133	652
D2233	415
D3333	671
D1212	760
D1313	760
D2323	128

Appendix C

Density of the fibre reinforced concrete and results from the beam test

Density of concrete

Specimen	Dry weight [g]	Volume [cm^3]	Density ρ [kg/m^3]
Cylinder 1	3940.9	1525.6	2583.2
Cylinder 2	3942.0	1540.1	2559.6
Cylinder 3	3952.9	1534.9	2575.4
Cylinder 4	3941.3	1537.1	2564.1
Cylinder 5	3982.5	1540.6	2585.0
Cylinder 6	3996.7	1557.9	2565.4
Average	**3959.4**	**1539.4**	**2572.1**

Results from beam test

Beam 1:

Av. Length [mm]	500.0
Av. Width [mm]	149.0
Av. Height [mm]	121.0

δ [mm]	CMOD_j [mm]	F_j [kN]	f_R,j [N/mm^2]
0.4615	0.5	12.24	4.21
1.2705	1.5	13.45	4.62
2.1700	2.5	13.83	4.75
3.0200	3.5	14.16	4.87

Plate 1:

x [mm]	5
Av. Length [mm]	450
Av. Width [mm]	147
Av. Height [mm]	54

δ [mm]	φ_3	CMOD_j [mm]	F_j [kN]	f_R,j [N/mm^2]
1.017	0.009	0.5	0.989	1.56
3.059	0.028	1.5	0.660	1.04
5.096	0.046	2.5	0.622	0.98

Plate 2:

x [mm]	66.5
Av. Length [mm]	450
Av. Width [mm]	55.25
Av. Height [mm]	151.25

δ [mm]	φ_3	CMOD_j [mm]	F_j [kN]	f_R,j [N/mm^2]
0.717	0.009	0.5	1.808	2.64
2.155	0.027	1.5	1.331	1.95
3.586	0.045	2.5	1.143	1.67

Plate 3:

x [mm]	33.5
Av. Length [mm]	450
Av. Width [mm]	52.5
Av. Height [mm]	146

δ [mm]	φ_3	CMOD_j [mm]	F_j [kN]	f_R,j [N/mm^2]
0.912	0.010	0.5	3.027	5.08
2.738	0.029	1.5	2.404	4.03
4.495	0.047	2.5	2.232	3.74

Appendix D

Results from numerical analyses

ABAQUS refers to the analyses done with the shear stiffness obtained in the shear test, ABAQUS FCA refers to the analyses done with an "infinite" stiffness.

Frequency analysis

	ABAQUS	ABAQUS FCA
Mode 1	11.719	11.990
Mode 2	18.648	37.107
Mode 3	34.261	34.850
Mode 4	39.098	51.250
Mode 5	51.170	51.890

All values in Hz.

Deflection analysis

	ABAQUS			ABAQUS FCA		
	Beam N	Beam S	Concrete span	Beam N	Beam S	Concrete span
Load case 1	0.2393	0.2393		0.2039	0.2039	
Load case 2	0.3497	0.1253		0.2938	0.1080	
Load case 3	0.2383	0.2383	0.0162	0.2014	0.2014	0.016

All values in mm.